ACCELERATING DARK ENERGY MODELS OF THE UNIVERSE IN ANISOTROPIC BIANCHI TYPE SPACE-TIMES AND RECENT OBSERVATIONS

A. Pradhan[1],*, *B. Saha*[2],**

[1] Department of Mathematics, Institute of Applied Sciences and Humanities,
G. L. A. University, Uttar Pradesh, India
[2] Joint Institute for Nuclear Research, Dubna

*E-mail: pradhan.anirudh@gmail.com
**E-mail: bijan@jinr.ru

ACCELERATING DARK ENERGY MODELS OF THE UNIVERSE IN ANISOTROPIC BIANCHI TYPE SPACE-TIMES AND RECENT OBSERVATIONS

A. Pradhan[1],*, B. Saha[2],**

[1] Department of Mathematics, Institute of Applied Sciences and Humanities,
G. L. A. University, Uttar Pradesh, India

[2] Joint Institute for Nuclear Research, Dubna

Motivated by the increasing evidence for the need of a geometry that resembles the Bianchi morphology to explain the observed anisotropy in the WMAP data, we have discussed some features of the Bianchi-type universes in the presence of a fluid that wields an anisotropic equation-of-state (EoS) parameter in general relativity. Such models are of great interest in cosmology in favor of constructing more realistic models than the FLRW models with maximally symmetric spatial geometry. Additionally, the interest in such models was promoted in recent years due to the debate that is going around the analysis and the interpretation of the WMAP data [21, 111, 112], whether they need a Bianchi-type morphology to be explained successfully [7, 103, 117, 118]. The ILC−WMAP data maps show seven axes well aligned with one another and the Virgo direction. For this reason, the Bianchi models are important in the study of anisotropies.

In the present study of Bianchi type-I, II, III, V and VI_0 space-times, we observe that the EoS for dark energy ω is found to be time-dependent and its existing range for derived models is in good agreement with the recent observations of SNe Ia data [50], SNe Ia data with CMBR anisotropy and galaxy clustering statistics [11] and the latest combination of cosmological datasets coming from CMB anisotropies, luminosity distances of high redshift type Ia supernovae and galaxy clustering [21, 51]. It has been suggested that the dark energy that explains the observed accelerating expansion of the Universe may arise due to the contribution to the vacuum energy of the EoS in a time-dependent background. The cosmological constant Λ is found to be a positive decreasing function of time and it approaches to a small positive value at late time (i.e., the present epoch) which is corroborated by results from recent type Ia supernovae observations.

Побуждаемые возрастающей потребностью в геометрии, сходной по структуре со структурами Бианки, для того чтобы объяснить наблюдаемую анизотропию в данных WMAP, мы рассмотрели некоторые свойства вселенных типа Бианки в присутствии материи, удовлетворяющей анизотропному уравнению состояния (EoS) в общей теории относительности. Такие модели очень интересны в космологии для построения

---

*E-mail: pradhan.anirudh@gmail.com

**E-mail: bijan@jinr.ru

более реалистичных моделей, чем FLRW с максимально симметричной пространственной геометрией. Более того, интерес к таким моделям возрос в последние годы благодаря обсуждению необходимости привлечения структур Бианки для анализа и интерпретации данных WMAP [21, 111, 112] для успешного их объяснения [103, 7, 118, 117]. Данные ILC−WMAP показывают семь направлений, хорошо согласованных друг с другом в направлении Девы. По этой причине модели Бианки столь важны для изучения анизотропии.

В данной работе в рамках Bianchi type-I, II, III, V и VI$_0$ мы наблюдаем, что EoS для темной энергии ω зависит от времени и его диапазон для этих моделей хорошо согласуется с недавними наблюдениями SNe I [50], SNe Ia с анизотропией микроволнового излучения, статистикой кластеризации галактик и новейшей комбинацией данных анизотропии микроволнового излучения, а также расстояний, определяемых по светимости [11], для сверхновых типа Ia в галактиках с большим красным смещением [51, 21]. Было предложено, что темная энергия, объясняющая видимое ускорение расширения Вселенной, может возникнуть за счет вклада вакуумной энергии Eos на фоне зависимости от времени. Оказалось, что космологическая постоянная Λ убывает со временем и при больших временах (в настоящее время) стремится к малому положительному значению, что подтверждается результатами недавних наблюдений сверхновой Ia.

PACS: 98.80.Es; 98.80-k; 95.36.+x

INTRODUCTION

The concept of dark energy (DE) was first invoked in the late 1990s by studying the brightness of distinct supernovae-exploding stars. In 1998, published observations of type Ia supernovae by the High-z Supernova Search Team [1] followed in 1999 by Supernova Cosmology Project [2, 3] suggested that the expansion of the Universe is accelerating. Recent observations of SNe Ia of high confidence level [4–6] have further confirmed this. In addition, measurements of the Cosmic Microwave Background (CMB) anisotropies [7–9], Large Scale Structure (LSS) [10–12], the Sloan Digital Sky Survey (SDSS) [13, 14], the Wilkinson Microwave Anisotropy Probe (WMAP) [15], and the Chandra X-ray observatory [16] strongly indicate that our Universe is dominated by a component with negative pressure, dubbed as dark energy, which constitutes with $\simeq 3/4$ of the critical density. The cosmic acceleration is realized with negative pressure and positive energy density which violate the strong energy condition. This violation gives a reverse gravitational effect. Due to this effect, the Universe gets a jerk, and the transition from the earlier deceleration phase to the recent acceleration phase takes place [17]. A recent survey of more than $200,000$ galaxies appears to confirm the existence of dark energy, although the exact physics behind it remains unknown [18].

During the last few years we are witnessing how cosmology is rapidly becoming an experimental branch of physics. It is no longer a pure realm of

philosophical speculation; theoretical models can be tested, and new and more accurate data in the near future will restrict our conceptions of the Universe to within few percent accuracy. The simplest candidate for the dark energy is the cosmological constant [19–22] which suffers from conceptual problems such as fine-tuning and coincidence problems [23]. Other scenarios include, Quintessence [24, 25], Chameleon [26], K-essence [27, 28], which is based on the earlier work of K-inflation [29], modified gravity [30–36], Tachyon [37] arising in string theory [38], Quintessential inflation [39], Chaplygin gas as well as generalized Chaplygin gas [40–45], cosmological nuclear energy [46]. In spite of these attempts, still cosmic acceleration is a challenge to modern cosmology and modern astrophysics.

High-precision measurements of expansion of the Universe are required to understand how the expansion rate changes over time. In general relativity, the evolution of the expansion rate is parameterized by the cosmological equation of state (the relationship between temperature, pressure, and combined matter, energy, and vacuum energy density for any region of space). Measuring the equation of state for dark energy is one of the biggest efforts in observational cosmology today. The DE model has been characterized in a conventional manner by the equation-of-state (EoS) parameter $\omega(t) = p/\rho$ which is not necessarily constant, where ρ is the energy density, and p is the fluid pressure [47]. The present data seem to slightly favour an evolving dark energy with EoS $\omega < -1$ around the present epoch and $\omega > -1$ in the near past. Obviously, ω cannot cross -1 for quintessence or phantom alone. Some efforts have been made to build a dark energy model whose EoS can cross the phantom divide. The simplest DE candidate is the vacuum energy ($\omega = -1$), which is mathematically equivalent to the cosmological constant (Λ). The other conventional alternatives, which can be described by minimally coupled scalar fields, are quintessence ($\omega > -1$) [48], phantom energy ($\omega < -1$) [49] and quintom (that can across from phantom region to quintessence region as evolved) and have time-dependent EoS parameter. Some other limits obtained from observational results coming from SNe Ia data [50] and combination of SNe Ia data with CMBR anisotropy and galaxy clustering statistics [10] are $-1.67 < \omega < -0.62$ and $-1.33 < \omega < -0.79$, respectively. The latest results in 2009, obtained after a combination of cosmological datasets coming from CMB anisotropies, luminosity distances of high-redshift type Ia supernovae and galaxy clustering, constrain the dark energy EoS to $-1.44 < \omega < -0.92$ at 68% confidence level [21, 51]. However, it is not at all obligatory to use a constant value of ω. Due to a lack of the observational evidence in making a distinction between constant and variable ω, usually the equation-of-state parameter is considered as a constant [52–54] with the phase wise value $-1, 0, -1/3$ and $+1$ for vacuum fluid, dust fluid, radiation and stiff dominated universe, respectively. But in general, ω is a function of time or redshift z or scale factor a, as well [25, 55, 56]. The redshift dependence of ω can

be linear like $\omega(z) = \omega_0 + \omega' z$, with $\omega' = \left.\dfrac{d\omega}{dz}\right|_{z=0}$ (see Huterer and Turner [57]; Weller and Albrecht [58]) or nonlinear as $\omega(z) = \omega_0 + \dfrac{\omega_1 z}{1+z}$ (Chavellier and Polarski [59]; Linder [60]). So, as far as the scale factor dependence of ω is concerned, the parameterization $\omega(a) = \omega_0 + \omega_a(1-a)$, where ω_0 is the present value $(a = 1)$, and ω_a is the measure of the time variation ω', is widely used in the literature [61]. Some literature are also available on the models with varying fields, such as cosmological models with variable EoS parameter in Kaluza–Klein metric and wormholes [48, 62]. In recent years, various forms of time-dependent ω have been used for variable Λ models by Mukhopadhyay et al. [63]. Setare [64–66] and Setare & Saridakis [67–69] have also studied the DE models in different contexts. Recently, dark energy models with variable EoS parameter have been studied by Ray et al. [70], Akarsu and Kilinc [71–74], Yadav et al. [75], Yadav and Yadav [76], Yadav and Saha [77], Pradhan and Amirhashchi [78, 79], Pradhan et al. [80–82], Amirhashchi et al. [83–86], Kumar [87, 88], Kumar and Akarsu [89], Kumar and Yadav [90], and Kumar and Singh [91]. In the well-known reviews on modified gravity [92, 93], it is clearly indicated that any modified gravity may be represented as effective fluid with time-dependent ω. The dark energy universe EoS with inhomogeneous, Hubble [95] parameter-dependent term is considered by Nojiri and Odintsov [94]. Later on, Nojiri and Odintsov [95] have also presented the late-time cosmological consequences of dark energy with time-dependent periodic EoS in oscillating universe.

After the discovery of General Theory of Relativity, a number of scientists including Einstein tried to apply the new gravitational dynamics to the Universe as a whole. This requires an assumption about the distribution of matter in the universe. One of the simplest assumptions is called the cosmological principle. It states that the Universe is homogeneous and isotropic on large distance scales. This implies that after averaging over sufficiently large distances, the universe would appear the same everywhere and in every direction. Today, there is considerable evidence, which suggests that the Universe may be isotropic and homogeneous. The best evidence for the isotropy of the observed Universe is the Cosmic Microwave Background (CMB) radiation. After discovery of CMB radiation, cosmology became a precision science. The CMB radiation is also considered to be a major experimental evidence on which the most commonly accepted theory about the origin of Universe, i.e., Big-Bang cosmology, is based.

Statistical Isotropy (SI) is usually assumed in almost all CMB studies. But, now, there exist many indications which suggest that CMB may violate this assumption. Apart from the CMB, there are some other indications of violation of SI which suggest the existence of a preferred direction in the Universe. These indications include distributions of polarizations from radiogalaxies (Birch [96];

Jain & Ralston [97]; Jain et al. [98]) and statistics of optical polarizations from quasars (Hutsemékers [99]; Hutsemékers & Lamy [100]; Jain et al. [98]; Ralston & Jain [101]). Polarization of electromagnetic waves coming from distant radio-galaxies and quasars measured at radio- and optical frequencies, respectively, are not consistent with the assumptions of SI, rather radiopolarizations are organized coherently over the dome of the sky, and optical polarizations are aligned in a preferential direction on very large scales, violating the assumed isotropy of the Universe. This confirmed strong significance of anisotropy and also claimed that the statistics are not consistent with isotropy at 99.9% confidence level. CMB anisotropies contain a wealth of information about the global properties of the Universe, like SI. It has been observed that the quadrupole and the octopole have almost all their power perpendicular to a common axis in space pointing towards Virgo cluster. The dipole, which is commonly attributed to our motion relative to the CMB rest frame, also aligns in the same direction as quadrupole and octopole. All these CMB axes point towards Virgo. The alignment of all these three axes nearly in the same direction is not expected under the condition of statistical isotropy (Tegmark et al. [102]; de Oliveira-Costa et al. [103]). There is also an indication of the large scale anisotropy in the distribution of galaxies. This is found in several subsets of the Sloan Digital Sky Survey (SDSS) data sample. The preferred direction in this case is found to depend significantly on the data sample used. Several authors have also searched for anisotropy using the supernova data set. Jain et al. [104] found violation of isotropy in this data. However, this could be attributed to selection effects. Using this data, Jain et al. [104] constrained the parameters of an anisotropic model which describes a universe with rotation and expansion. A recent analysis (Cooke & Lynden-Bell [105]) finds a signal with very low significance with axis roughly towards CMB dipole. Subsequently there have been a large number of studies which claim the CMB is not consistent with isotropy. The possible violation of SI in CMB has led to many theoretical studies. In recent years, there have been a large number of studies which claim the CMB temperature fluctuations are not consistent with statistical isotropy and are questioning the cosmological principle. Some authors have investigated the possibility that dark energy is anisotropic (see Cooray, Holz & Caldwell [106] and references therein). Basing on these studies, one may not preclude the possibility of our Universe being anisotropic. However, with such optimistic objectives, these studies will require a dedicated all-sky survey to search for SNe. Recently, the dipole at the cluster locations was calculated using the same techniques for WMAP and Planck [107]. The authors found a dark-flow signal which correlates with X-ray properties and is, therefore, likely related to cluster gas, and not to the primary CMB, foregrounds or noise. The results are in excellent agreement with their earlier findings and are consistent both with WMAP 9-year and with Planck 1-year ones. The March 2013 release of Planck data was another milestone in the fast-paced series of advances in observational

cosmology. The consistency of the nine-year WMAP data and the first-release Planck data was examined in [108]. Sky maps, power spectra, and the inferred ΛCDM cosmological parameters were compared. Residual dipoles are seen in the WMAP and Planck sky map differences, but their amplitudes are consistent within the quoted uncertainties, and they are not large enough to explain the widely-noted differences in angular power spectra at higher l [108].

The Bianchi universes form almost complete class of spatially homogeneous but not necessarily isotropic relativistic cosmological models. They provide generalization of the standard Friedmann–Lemaître (FL) models, which are based on the spatially homogeneous and isotropic Robertson–Walker (RW) metrics [109, 110]. Such models are of great interest in cosmology in favour of constructing more realistic models than FLRW models with maximally symmetric spatial geometry. Namely, although the observed universe seems to be almost isotropic on large scales, the early and/or very late universe could be anisotropic [109]. Additionally, the interest in such models was promoted in recent years due to the debate that is going around the analysis and the interpretation of the WMAP [20, 105–107] data, whether they need a Bianchi type morphology to be explained successfully [7, 108–112].

This review article is organized as follows. In the next Section we set up the formalism of a Bianchi type-I anisotropic dark-energy model. In Sec. 2, we derive the LRS Bianchi type-II dark-energy models. Section 3 deals with dark-energy models in anisotropic Bianchi type-III space-time. In Sec. 4, we discuss the accelerating dark-energy models in Bianchi type-V space-time. Section 5 deals with accelerating dark-energy models with anisotropic fluid in Bianchi type-VI$_0$ space-time. In the last Section we draw our conclusions.

1. BIANCHI TYPE-I ANISOTROPIC DARK-ENERGY MODELS

We consider totally anisotropic Bianchi type-I line element, given by

$$ds^2 = -dt^2 + A^2 \, dx^2 + B^2 \, dy^2 + C^2 \, dz^2, \tag{1}$$

where the metric potentials A, B, and C are functions of t alone. This ensures that the model is spatially homogeneous.

The simplest generalization of Equation-of-State (EoS) parameter of perfect fluid may be to determine the EoS parameter separately on each spatial axis by preserving the diagonal form of the energy momentum tensor in a consistence way with the considered metric. Therefore, the energy momentum tensor of fluid is taken as

$$T_i^j = \text{diag} \, [T_0^0, T_1^1, T_2^2, T_3^3]. \tag{2}$$

Thus, one may parameterize it as follows:

$$T_i^j = \text{diag}\,[\rho, -p_x, -p_y, -p_z] = \text{diag}\,[1, -\omega_x, -\omega_y, -\omega_z]\rho =$$
$$= \text{diag}\,[1, -\omega, -(\omega + \delta), -(\omega + \gamma)]\rho. \quad (3)$$

Here p_x, p_y, and p_z are the pressures; ρ is the proper energy density; and ω_x, ω_y, and ω_z are the directional EoS parameters along the x, y, and z axes, respectively. The ω is the deviation-free EoS parameter of the fluid. We have parameterized the deviation from isotropy by setting $\omega_x = \omega$ and then introducing skewness parameters δ and γ that are the deviations from ω along the y and z axes, respectively.

Einstein's field equations (with gravitational units, $8\pi G = 1$ and $c = 1$) read as

$$R_i^j - \frac{1}{2}Rg_i^j = T_i^j, \quad (4)$$

where the symbols have their usual meaning. In a comoving co-ordinate system, Einstein's field equation (4), with (3) for B-I metric (1), subsequently leads to the following system of equations:

$$\frac{\ddot{B}}{B} + \frac{\ddot{C}}{C} + \frac{\dot{B}\dot{C}}{BC} = -\omega\rho, \quad (5)$$

$$\frac{\ddot{C}}{C} + \frac{\ddot{A}}{A} + \frac{\dot{C}\dot{A}}{CA} = -(\omega + \delta)\rho, \quad (6)$$

$$\frac{\ddot{A}}{A} + \frac{\ddot{B}}{B} + \frac{\dot{A}\dot{B}}{AB} = -(\omega + \gamma)\rho, \quad (7)$$

$$\frac{\dot{A}\dot{B}}{AB} + \frac{\dot{B}\dot{C}}{BC} + \frac{\dot{C}\dot{A}}{CA} = \rho. \quad (8)$$

Here and in what follows an over dot denotes ordinary differentiation with respect to t.

The spatial volume for model (1) is given by

$$V^3 = ABC. \quad (9)$$

We define $a = (ABC)^{1/3}$ as the average scale factor so that the Hubble parameter is anisotropic and may be defined as

$$H = \frac{\dot{a}}{a} = \frac{1}{3}\left(\frac{\dot{A}}{A} + \frac{\dot{B}}{B} + \frac{\dot{C}}{C}\right). \quad (10)$$

We define the generalized mean Hubble parameter H as

$$H = \frac{1}{3}(H_x + H_y + H_z), \quad (11)$$

where $H_x = \dot{A}/A$, $H_y = \dot{B}/B$ and $H_z = \dot{C}/C$ are the directional Hubble parameters in the directions of x, y, and z, respectively.

An important observational quantity is the deceleration parameter q, which is defined as

$$q = -\frac{a\ddot{a}}{\dot{a}^2}. \tag{12}$$

The scalar expansion θ, shear scalar σ^2 and the average anisotropy parameter A_m are defined by

$$\theta = \frac{\dot{A}}{A} + \frac{\dot{B}}{B} + \frac{\dot{C}}{C}, \tag{13}$$

$$\sigma^2 = \frac{1}{2}\left(\sum_{i=1}^{3} H_i^2 - \frac{1}{3}\theta^2\right), \tag{14}$$

$$A_m = \frac{1}{3}\sum_{i=1}^{3}\left(\frac{\triangle H_i}{H}\right)^2, \tag{15}$$

where $\triangle H_i = H_i - H$ $(i = 1, 2, 3)$.

The field equations (5)–(8) are a system of four equations with seven unknown parameters A, B, C, ρ, ω, δ, and γ. Three additional constraints relating these parameters are required to obtain explicit solutions of the system.

Einstein's field equations are a coupled system of highly nonlinear differential equations and we seek physical solution to the field equations for their applications in cosmology and astrophysics. In order to solve the field equations, we normally assume a form for the matter content or the space-time admits killing vector symmetries. Solutions to the field equations may also be generated by applying a law of variation for the Hubble parameter proposed by Berman [119]. Firstly, we apply the special law of variation for the generalized Hubble parameter that yields a constant value of deceleration parameter. Since the line element (1) is completely characterized by the Hubble parameter H, therefore, let us consider that the mean Hubble parameter H is related to the average scale factor a by the relation

$$H = \ell a^{-n} = \ell(ABC)^{-n/3}, \tag{16}$$

where $\ell(> 0)$ and $n(\geqslant 0)$ are constants. Such a type of relations has already been considered by Berman [119], Berman and Gomide [120] for solving FRW models. Later on, many authors (see, Singh et al. [121–123], Pradhan and Jotania [124] and references therein) have studied the flat FRW and Bianchi-type models by using the special law for the Hubble parameter that yields a constant value of deceleration parameter.

From (10) and (16), we get

$$\dot{a} = \ell a^{-n+1} \tag{17}$$

and

$$\ddot{a} = -\ell^2(n-1)a^{-2n+1}. \tag{18}$$

Substituting (17) and (18) into (12), we get

$$q = n - 1. \tag{19}$$

We observe that relation (19) gives q as a constant. The sign of q indicates whether the model inflates or not. The positive sign of q, i.e. $(n > 1)$ corresponds to the "standard" decelerating model, whereas the negative sign of q, i.e., $0 \leqslant n < 1$ indicates acceleration. It is remarkable to mention here that though the current observations of SNe Ia and CMBR favour accelerating models ($q < 0$), but both do not altogether rule out the decelerating ones which are also consistent with these observations (see, Vishwakarma [125]).

Integrating Eq. (17), we obtain the law of average scale factor "a" as

$$a = (n\ell t + c_1)^{1/n} \quad \text{for} \quad n \neq 0 \tag{20}$$

and

$$a = c_2\, e^{\ell t} \quad \text{for} \quad n = 0, \tag{21}$$

where c_1 and c_2 are constants of integration. Thus, the law (16) provides two types of the expansion in the Universe, i.e., (i) power-law (20) and (ii) exponential-law (21).

Secondly, we assume that the component σ_1^1 of the shear tensor σ_i^j is proportional to the expansion scalar (θ), i.e., $\sigma_1^1 \propto \theta$. This condition leads to the following relation between the metric potentials:

$$A = (BC)^m, \tag{22}$$

where m is a positive constant. The motive behind assuming this condition is explained with reference to Thorne [126], the observations of the velocity–redshift relation for extragalactic sources suggest that the Hubble expansion of the Universe is isotropic today within $\approx 30\%$ (Kantowski and Sachs [127]; Kristian and Sachs [128]). To put more precisely, redshift studies place the limit,

$$\frac{\sigma}{H} \leqslant 0.3,$$

on the ratio of shear σ to the Hubble constant H in the neighbourhood of our Galaxy today. Collins et al. [129] have pointed out that for spatially homogeneous metric, the normal congruence to the homogeneous expansion satisfies the condition σ/θ to be constant.

Thirdly, we assume that the deviations from ω along y and z axes are the same, i.e., $\gamma = \delta$.

Subtracting (6) from (7) and taking integral of the resulting equation two times, we get

$$\frac{B}{C} = c_3 \exp\left[c_4 \int (ABC)^{-1} dt\right],\tag{23}$$

where c_3 and c_4 are constants of integration.

After solving the field equations (5)–(8) for the power-law volumetric expansion (20) by considering Eqs. (22) and (23), we obtain the scale factors as follows:

$$A(t) = (n\ell t + c_1)^{\frac{3m}{n(m+1)}},\tag{24}$$

$$B(t) = \sqrt{c_3}(n\ell t + c_1)^{\frac{3}{2n(m+1)}} \exp\left[\frac{c_4}{2\ell(n-3)}(n\ell t + c_1)^{\frac{n-3}{n}}\right],\tag{25}$$

$$C(t) = \frac{1}{\sqrt{c_3}}(n\ell t + c_1)^{\frac{3}{2n(m+1)}} \exp\left[-\frac{c_4}{2\ell(n-3)}(n\ell t + c_1)^{\frac{n-3}{n}}\right],\tag{26}$$

provided $n \neq 3$.

Hence the model (1) is reduced to

$$ds^2 = -dt^2 + (n\ell t + c_1)^{\frac{6m}{n(m+1)}} dx^2 + c_3(n\ell t + c_1)^{\frac{3}{n(m+1)}} \times$$

$$\times \exp\left[\frac{c_4}{\ell(n-3)}(n\ell t + c_1)^{\frac{n-3}{n}}\right] dy^2 +$$

$$+ \frac{1}{c_3}(n\ell t + c_1)^{\frac{3}{n(m+1)}} \exp\left[-\frac{c_4}{\ell(n-3)}(n\ell t + c_1)^{\frac{n-3}{n}}\right] dz^2.\tag{27}$$

The rate of expansion H_i in the direction of x, y, and z reads as

$$H_x = \frac{3m\ell}{m+1}(n\ell t + c_1)^{-1},\tag{28}$$

$$H_y = \frac{3\ell}{2(m+1)}(n\ell t + c_1)^{-1} + \frac{1}{2}c_4(n\ell t + c_1)^{-\frac{3}{n}},\tag{29}$$

$$H_z = \frac{3\ell}{2(m+1)}(n\ell t + c_1)^{-1} - \frac{1}{2}c_4(n\ell t + c_1)^{-\frac{3}{n}}.\tag{30}$$

The Hubble parameter H, scalar of expansion θ, shear scalar σ, and the average anisotropy parameter A_m for the model (27) are obtained as

$$\theta = 3H = 3\ell(n\ell t + c_1)^{-1},\tag{31}$$

$$\sigma^2 = \frac{3\ell^2(2m-1)^2}{2(m+1)^2}(n\ell t + c_1)^{-2} + \frac{1}{4}c_4^2(n\ell t + c_1)^{-\frac{6}{n}},\tag{32}$$

$$A_m = \frac{(2m-1)^2}{(m+1)^2} + \frac{c_4^2}{6\ell^2}(n\ell t + c_1)^{\frac{2(n-3)}{n}}. \tag{33}$$

The energy density of the fluid can be find by using Eqs. (24)–(26) in (8)

$$\rho = \frac{9\ell^2(4m+1)}{4(m+1)^2}(n\ell t + c_1)^{-2} - \frac{1}{4}c_4^2(n\ell t + c_1)^{-\frac{6}{n}}. \tag{34}$$

Using Eqs. (25), (26), and (34) in (5), the EoS parameter ω is obtained as

$$\omega = \frac{3\ell^2 \left[\dfrac{-4n(m+1)+9}{(m+1)^2}\right](n\ell t + c_1)^{-2} + c_4^2(n\ell t + c_1)^{-\frac{6}{n}}}{c_4^2(n\ell t + c_1)^{-\frac{6}{n}} - \dfrac{9\ell^2(4m+1)}{(m+1)^2}(n\ell t + c_1)^{-2}}. \tag{35}$$

Using Eqs. (24)–(26), (34), and (35) in either (6) or (7), the skewness parameters δ and γ (i.e., deviation from ω along y-axis and z-axis) are computed as

$$\delta = \gamma = \frac{\dfrac{3\ell^2(3-n)[4mn(m+1)-3]}{n(m+1)^2}(n\ell t + c_1)^{-2}}{c_4^2(n\ell t + c_1)^{-\frac{6}{n}} - \dfrac{9\ell^2(4m+1)}{(m+1)^2}(n\ell t + c_1)^{-2}}. \tag{36}$$

If the present work is compared with the experimental results already mentioned in Introduction, then one can conclude that the limit of ω provided by Eq. (35) may be accommodated with the acceptable range of the EoS parameter. Also it is observed that at $t = t_c$, ω vanishes, where t_c is a critical time given by

$$t_c = \frac{1}{n\ell}\left(\frac{\ell\sqrt{3[4n(m+1)-9]}}{c_4(m+1)}\right)^{\frac{n}{n-3}} - \frac{c_1}{n\ell}. \tag{37}$$

Thus, for this particular time our model represents a dusty universe. We note that the earlier real matter at $t \leqslant t_c$, where $\omega \geqslant 0$, later on at $t > t_c$, where $\omega < 0$, converted to the dark energy dominated phase of universe.

For the value of ω to be consistent with observation [50], we have the following general condition:

$$t_1 < t < t_2, \tag{38}$$

where

$$t_1 = \frac{1}{n\ell}\left[1.12\ell\frac{\sqrt{4n(m+1)+5(4m+1)}}{c_4(m+1)}\right]^{\frac{n}{n-3}} - \frac{c_1}{n\ell} \tag{39}$$

and

$$t_2 = \frac{1}{n\ell}\left[1.36\ell\frac{\sqrt{4n(m+1)+7.44m-7.14}}{c_4(m+1)}\right]^{\frac{n}{n-3}} - \frac{c_1}{n\ell}. \tag{40}$$

For this constraint we obtain $-1.67 < \omega < -0.62$, which is in good agreement with the limit obtained from observational results coming from SNe Ia data (Knop et al. [50]).

For the value of ω to be consistent with observation [10], we have the following general condition:

$$t_3 < t < t_4, \tag{41}$$

where

$$t_3 = \frac{1}{n\ell} \left[1.35\ell \frac{\sqrt{4n(m+1) + 15.96m - 5.01}}{c_4(m+1)} \right]^{\frac{n}{n-3}} - \frac{c_1}{n\ell} \tag{42}$$

and

$$t_4 = \frac{1}{n\ell} \left[1.3\ell \frac{\sqrt{4n(m+1) + 9.48m - 6.63}}{c_4(m+1)} \right]^{\frac{n}{n-3}} - \frac{c_1}{n\ell}. \tag{43}$$

For this constraint, we obtain $-1.33 < \omega < -0.79$, which is in good agreement with the limit obtained from observational results coming from SNe Ia data with CMB anisotropy and galaxy clustering statistics (Tegmark et al. [10]).

For the value of ω to be consistent with the latest observations in 2009 [21, 51], we have the following general condition:

$$t_5 < t < t_6, \tag{44}$$

where

$$t_5 = \frac{1}{n\ell} \left[1.6\ell \frac{\sqrt{4n(m+1) + 17.28m - 4.68}}{c_4(m+1)} \right]^{\frac{n}{n-3}} - \frac{c_1}{n\ell} \tag{45}$$

and

$$t_6 = \frac{1}{n\ell} \left[1.25\ell \frac{\sqrt{4n(m+1) + 11.04m - 6.24}}{c_4(m+1)} \right]^{\frac{n}{n-3}} - \frac{c_1}{n\ell}. \tag{46}$$

For this constraint, we obtain the dark energy EoS to $-1.44 < \omega < -0.92$, which is in good agreement with the limit of the latest observational result in 2009 at 68% confidence level (Hinshaw et al. [51]; Komatsu et al. [21]).

We also observe that if

$$t_0 = \frac{1}{n\ell} \left[1.22\ell \frac{\sqrt{4n(m+1) + 6(2m-1)}}{c_4(m+1)} \right]^{\frac{n}{n-3}} - \frac{c_1}{n\ell}, \tag{47}$$

then for $t = t_0$, $\omega = -1$ (i.e., cosmological constant dominated universe), for $t < t_0$, $\omega > -1$ (i.e., quintessence), and for $t > t_0$, $\omega < -1$ (i.e., super quintessence or phantom fluid dominated universe) (Caldwell [49]).
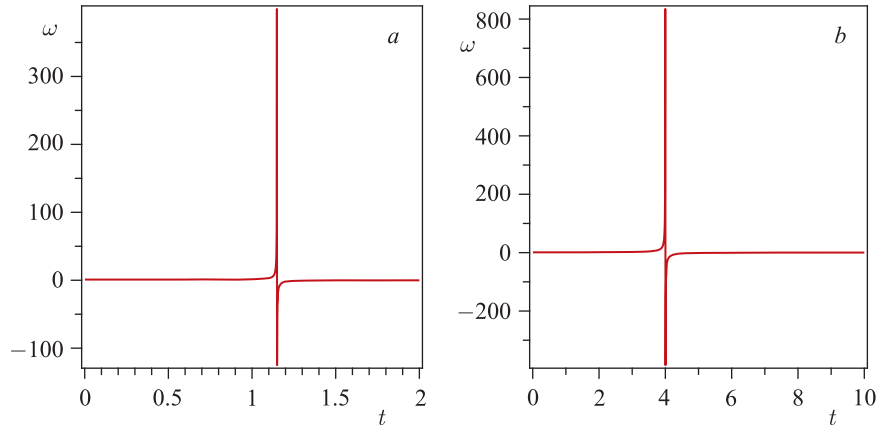
Fig. 1. *a*) The EoS parameter ω versus t in power-law expansion for $q < 0$. Here $\ell = 0.33$, $n = 0.5$, $m = 2$, $c_4 = 2$. *b*) The EoS parameter ω versus t in power-law expansion for $q > 0$. Here $\ell = 0.33$, $n = 2$, $m = 2$, $c_4 = 2$

Figure 1, *a* and *b* depicts the variation of equation-of-state parameter (ω) versus cosmic time (t) in the two modes (i.e., $q < 0$ and $q > 0$) of evolution of the Universe, as a representative case with appropriate choice of constants of integration and other physical parameters using reasonably well-known situations. From Fig. 1, we conclude that in early stage of evolution of the Universe, the EoS parameter ω was positive (i.e., the Universe was matter dominated) and at late time it is evolving with negative value (i.e., at the present time). The earlier real matter later on converted to the dark-energy dominated phase of the universe in both accelerating and decelerating modes.

From Eq. (34), we note that energy density of the fluid $\rho(t)$ is a decreasing function of time and $\rho \geqslant 0$ when

$$t \geqslant \frac{1}{n\ell}\left[\left(\frac{c_4(m+1)}{3\ell\sqrt{4m+1}}\right)^{\frac{n}{3-n}} - c_1\right]. \tag{48}$$

Figure 2, *a* and *b* presents the plots of energy density of the fluid (ρ) versus time in accelerating and decelerating modes of the Universe, respectively. In both the modes, it is understood that in early Universe ρ is decreasing with time and at late time it approaches zero.

In absence of any curvature, matter energy density Ω_m and dark energy Ω_Λ are related by the equation

$$\Omega_m + \Omega_\Lambda = 1, \tag{49}$$
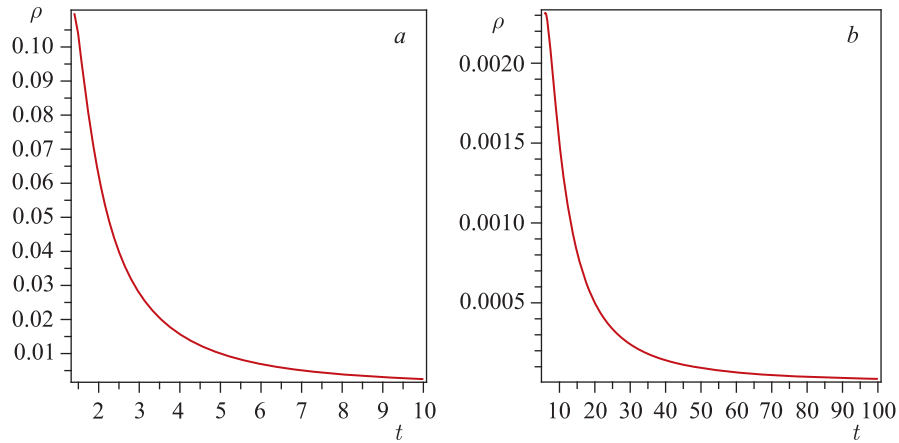
Fig. 2. *a*) The energy density ρ versus t in power-law expansion for $q < 0$. Here $\ell = 0.33$, $n = 0.5$, $m = 2$, $c_4 = 2$. *b*) The energy density ρ versus t in power-law expansion for $q > 0$. Here $\ell = 0.33$, $n = 2$, $m = 2$, $c_4 = 2$

where $\Omega_m = \dfrac{\rho}{3H^2}$ and $\Omega_\Lambda = \dfrac{\Lambda}{3H^2}$. Thus, Eq. (49) reduces to

$$\frac{\rho}{3H^2} + \frac{\Lambda}{3H^2} = 1. \tag{50}$$

Using Eqs. (31) and (34) in (50), the cosmological constant is computed as

$$\Lambda = \frac{3\ell^2(4m^2 - 4m + 1)}{4(m+1)^2}(n\ell t + c_1)^{-2} + \frac{1}{4}c_4^2(n\ell t + c_1)^{-\frac{6}{n}}. \tag{51}$$

From Eq. (51) we observe that Λ is a decreasing function of time and it is always positive for $m > 1/2$.

In recent time, the Λ-term has interested theoreticians and observers for various reasons. The nontrivial role of the vacuum in the early universe generates the Λ-term that leads to inflationary phase. Observationally, this term provides an additional parameter to accommodate conflicting data on the values of the Hubble constant, the deceleration parameter, the density parameter, and the age of the universe (for example, see the references Gunn and Tinsley [130]; Wampler and Burke [131]). The behaviour of the universe in this model will be determined by the cosmological term Λ, this term has the same effect as a uniform mass density $\rho_{\text{eff}} = -\Lambda$, which is constant in time. A positive value of Λ corresponds to a negative effective mass density (repulsion). Hence, we expect that in the universe with a positive value of Λ, the expansion will tend to accelerate, whereas in the universe with negative value of Λ the expansion will slow down, stop,

and reverse. In a universe with both matter and vacuum energy, there is a competition between the tendency of Λ to cause acceleration and the tendency of matter to cause deceleration with the ultimate fate of the universe depending on the precise amounts of each component. This continues to be true in the presence of spatial curvature, and with a nonzero cosmological constant it is no longer true that the negatively curved ("open") universes expand indefinitely while positively curved ("closed") universes will necessarily recollapse — each of the four combinations of negative or positive curvature and eternal expansion or eventual recollapse become possible for appropriate values of the parameters. There may even be a delicate balance, in which the competition between matter and vacuum energy is needed drawn and the universe is static (nonexpanding). *The search for such a solution was Einstein's original motivation for introducing the cosmological constant.* It is also remarkable to mention here that the dark energy that explains the observed accelerating expansion of the universe may arise due to the contribution to the vacuum energy of the EoS in a time-dependent background.

Figures 3, a and b are the plots of cosmological constant Λ versus time in accelerating and decelerating modes of the Universe, respectively. In both modes, we observe that cosmological parameter is a decreasing function of time and it approaches a small positive value at late time (i.e., at present epoch). Recent cosmological observations [1–3] suggest the existence of a positive cosmological constant Λ with the magnitude $\Lambda(G\hbar/c^3) \approx 10^{-123}$. These observations on magnitude and redshift of type Ia supernova suggest that our Universe may be an accelerating one with induced cosmological density through the cosmological Λ-term. But this does not rule out the decelerating ones which are also consistent with these observations (Vishwakarma [125]). Thus the nature of Λ in our derived DE model is supported by recent observations.

From Eqs. (28)–(33), it can be seen that the spatial volume is zero at $t = -c_1/n\ell$, and it increases with the cosmic time. The parameters H_i, H, θ, and σ diverge at the initial singularity. There is a point type singularity [132] at $t = -c_1/n\ell$ in the model. The mean anisotropic parameter is an increasing function of time for $n > 3$ whereas for $n < 3$ it decreases with time. Thus, the dynamics of the mean anisotropy parameter depends on the value of n. Since $\sigma^2/\theta^2 = \mathrm{const}$ (from early to late time), the model does not approach isotropy through the whole evolution of the universe.

The main features of the model are as follows:

• The DE model is based on exact solutions of the Einstein field equations for the anisotropic B-I space-time filled with perfect fluid with variable EoS parameter ω. The exact solutions of the Einstein field equations have been obtained by assuming power-law volumetric expansion in a way to cover the accelerating and decelerating phases of the universe. The derived DE models add one more feather to the literature.
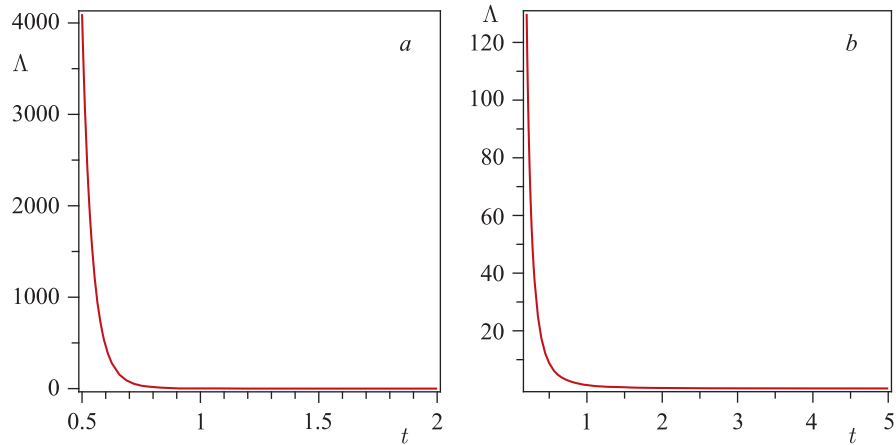
Fig. 3. *a*) The cosmological constant Λ versus t in power-law expansion for $q < 0$. Here $\ell = 0.33$, $n = 0.5$, $m = 2$, $c_4 = 2$. *b*) The cosmological constant Λ versus t in power-law expansion for $q > 0$. Here $\ell = 0.33$, $n = 2$, $m = 2$, $c_4 = 2$

- In both accelerating and decelerating phases of the universe, it is observed that, in early stage, the EoS parameter ω is positive, i.e., the universe was a matter dominated in early stage, but in late time, the universe is evolving with negative values, i.e., the present epoch (see, Fig. 1). Thus our DE model represents realistic model.

- The DE model presents the dynamics of EoS parameter ω provided by Eqs. (35) and may accommodate with the acceptable range with recent observations (Knop et al. [50]; Tegmark et al. [10]; Hinshaw et al. [51]; Komatsu et al. [21]). It is already observed and shown in the previous section that for different cosmic times, we obtain cosmological constant dominated universe, quintessence and phantom fluid dominated universe (Caldwell [102]), representing the different phases of the universe through out the evolving process. Unlike Robertson–Walker (RW) metric, Bianchi type metrics can admit a DE that yields an anisotropic EoS parameter according to the characteristics. The cosmological data — from the large-scale structures and type Ia supernovae observations — do not rule out the possibility of an anisotropic DE either [133, 134]. Therefore, one cannot rule out the possibility of anisotropic nature of DE at least in the framework of B-I space-time.

- Our DE model is of interest because the nature of decaying vacuum energy density $\Lambda(t)$ is supported by recent cosmological observations. These observations on magnitude and redshift of type Ia supernova suggest that our Universe may be an accelerating one with induced cosmological density through the cosmological Λ-term.

2. BIANCHI TYPE-II ANISOTROPIC DARK-ENERGY MODELS

We consider a homogeneous LRS Bianchi type-II space-time for which

$$ds^2 = \eta_{ij}\theta^i\theta^j, \qquad \eta_{ij} = (1,1,1,-1), \tag{52}$$

where the Cartan bases θ^i are given by

$$\theta^1 = A\,dx, \quad \theta^2 = B(dy + x\,dz), \quad \theta^3 = A\,dz, \quad \theta^4 = dt, \tag{53}$$

where A and B are functions of time only, since in LRS B-II, $T_1^1 = T_2^2 = T_3^3$ (see Saha [135]).

In a comoving co-ordinate system, the Einstein field equations (4) with (3) for LRS B-II metric subsequently lead to the following system of three independent equations:

$$\frac{\ddot{A}}{A} + \frac{\ddot{B}}{B} + \frac{\dot{A}\dot{B}}{AB} + \frac{1}{4}\frac{B^2}{A^4} = -\omega\rho, \tag{54}$$

$$2\frac{\ddot{A}}{A} + \frac{\dot{A}^2}{A^2} - \frac{3}{4}\frac{B^2}{A^4} = -\omega\rho, \tag{55}$$

$$2\frac{\dot{A}\dot{B}}{AB} + \frac{\dot{A}^2}{A^2} - \frac{1}{4}\frac{B^2}{A^4} = \rho, \tag{56}$$

where an over dot denotes ordinary differentiation with respect to t.

The spatial volume for LRS B-II is given by

$$V^3 = A^2 B. \tag{57}$$

We define $a = (A^2 B)^{1/3}$ as the average scale factor of LRS B-II model (52) so that the Hubble parameter is given by

$$H = \frac{\dot{a}}{a} = \frac{1}{3}\left(\frac{2\dot{A}}{A} + \frac{\dot{B}}{B}\right). \tag{58}$$

The field equations (54)−(56) are a system of three independent equations in five unknown parameters A, B, ρ, ω, δ, or γ. Two additional constraints relating these parameters are required to obtain explicit solutions of the system.

Firstly, we apply the variation law for the generalized Hubble parameter that yields a constant value of deceleration parameter $q = n - 1$. Following the technique as in B-I space-time, we obtain the law of average scale factor "a" as

$$a = (kt + c_0)^{1/n} \quad \text{for} \quad n \neq 0, \tag{59}$$

and

$$a = c_1 \, e^{Dt} \quad \text{for} \quad n = 0, \tag{60}$$

where $k = nD$, and c_0, c_1 are constants of integration.

Secondly, we assume that the expansion (θ) in the model is proportional to the shear scalar σ. This condition leads to

$$A = B^m, \tag{61}$$

where m is a constant.

In the following Subsecs. 2.1, 2.2, we consider two types of solutions, i.e., for power-law and exponential form volumetric expansion.

2.1. Case (i): When $n \neq 0$, i.e., Model for Power-Law Expansion. After solving the field equations (54)–(56) for the power-law volumetric expansion (59) by considering Eqs. (58) and (61), we obtain the expressions for metric coefficient as follows:

$$B = \ell(kt + c_0)^{\frac{1}{mr}}, \tag{62}$$

$$A = L(kt + c_0)^{\frac{1}{r}}, \tag{63}$$

where c_2 is an integrating constant and $\ell = c_2^{\frac{3}{2m+1}}$, $L = \ell^m$, $r = \dfrac{n(2m+1)}{3m}$.

Thus, the Hubble parameter H, scalar of expansion θ, shear scalar σ, and the average anisotropy parameter A_m are computed as

$$H = \frac{k}{n(kt + c_0)}, \tag{64}$$

$$\theta = 3H = \frac{3k}{n(kt + c_0)}, \tag{65}$$

$$\sigma^2 = \frac{(m-1)^2}{3m^2 r^2} \frac{k^2}{(kt + c_0)^2}, \tag{66}$$

$$A_m = \frac{n^2(2m^2 + 1)}{3m^2 r^2} - \frac{2n(2m + 1)}{3mr} + 1. \tag{67}$$

Equations (65) and (66) lead to

$$\frac{\sigma^2}{\theta^2} = \frac{n^2(m-1)^2}{27m^2 r^2}. \tag{68}$$

From the above results, it can be seen that the spatial volume is zero at $t = -c_0/k$, and it increases with the cosmic time. The parameters H, θ, and σ diverge at the initial singularity $t = -c_0/k$. There is a point type singularity at $t = -c_0/k$

(MacCallum [132]). The mean anisotropic parameter is uniform through the whole evolution of the universe. Thus, the dynamics of the mean anisotropy parameter does not depend on the cosmic time t. Since $\sigma^2/\theta^2 = $ const, the model does not approach isotropy through the whole evolution of the universe.

The energy density of the fluid and the deviation-free EoS parameter are obtained as

$$\rho = \frac{k^2(m+2)}{mr^2}\frac{1}{(kt+c_0)^2} - \frac{1}{4}\ell_0(kt+c_0)^{\frac{2-4m}{mr}}, \tag{69}$$

$$\omega = \frac{\dfrac{3}{4}\ell_0(kt+c_0)^{\frac{2-4m}{mr}} - \dfrac{k^2(3-2r)}{r^2}\dfrac{1}{(kt+c_0)^2}}{\dfrac{k^2(m+2)}{mr^2}\dfrac{1}{(kt+c_0)^2} - \dfrac{1}{4}\ell_0(kt+c_0)^{\frac{2-4m}{mr}}}, \tag{70}$$

where $\ell_0 = \ell^{2-4m}$.

So, if the present work is compared with experimental results already mentioned in Introduction, then one can conclude that the limit of ω given by (70) may accommodated with the acceptable range of EoS parameter. Also it is observed that for $t = t_c$, ω vanishes, where t_c is a critical time given by

$$t_c = \frac{1}{k}\left[\frac{4k^2(3-2r)}{3\ell_0 r^2}\right]^{\frac{mr}{2(mr-2m+1)}} - \frac{c_0}{k}. \tag{71}$$

Thus, for this particular time our model represents dusty universe. We also note that the earlier real matter at $t \leqslant t_c$, where $\omega \geqslant 0$, later on at $t > t_c$, where $\omega < 0$, converted to the dark energy dominated phase of universe as shown in Fig. 4.

For the value of ω to be consistent with observation (Knop et al. [50]), we have the following general condition for $n \neq 0$:

$$t_1 < t < t_2, \tag{72}$$

where

$$t_1 = \frac{1}{k}\left\{\frac{k^2[m(1.33-2r)-3.34]}{0.33m\ell_0 r^2}\right\}^{\frac{mr}{2(mr-2m+1)}} - \frac{c_0}{k} \tag{73}$$

and

$$t_2 = \frac{1}{k}\left\{\frac{k^2[m(2.38-2r)-1.24]}{0.6m\ell_0 r^2}\right\}^{\frac{mr}{2(mr-2m+1)}} - \frac{c_0}{k}. \tag{74}$$

For this constraint, the EoS parameter ω is restricted to the limit $-1.67 < \omega < -0.62$ which is exactly in good agreement with the limit obtained from observational results coming from SN Ia data (Knop et al. [50]).

For the value of ω to be consistent with observation (Tegmark et al. [10]), we have the following general condition for $n \neq 0$:

$$t_3 < t < t_4, \tag{75}$$
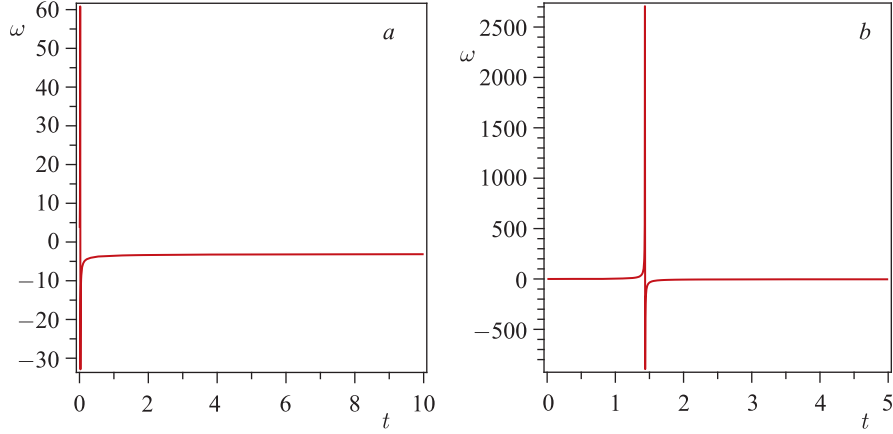
Fig. 4. *a*) The EoS parameter ω versus t in power-law expansion for $q < 0$. Here $\ell_0 = 1.3$, $r = 2$, $n = 0.5$, $m = 2$, $k = 0.35$. *b*) The EoS parameter ω versus t in power-law expansion for $q > 0$. Here $\ell_0 = 1.3$, $r = 2.7$, $n = 2$, $m = 0.5$, $k = 0.35$

where

$$t_3 = \frac{1}{k} \left\{ \frac{k^2[m(1.67 - 2r) - 2.66]}{0.44 m\ell_0 r^2} \right\}^{\frac{mr}{2(mr - 2m + 1)}} - \frac{c_0}{k} \tag{76}$$

and

$$t_4 = \frac{1}{k} \left\{ \frac{k^2[m(2.21 - 2r) - 1.58]}{0.55 m\ell_0 r^2} \right\}^{\frac{mr}{2(mr - 2m + 1)}} - \frac{c_0}{k}. \tag{77}$$

For this constraint, we obtain $-1.33 < \omega < -0.79$, which is in good agreement with the limit obtained from observational results coming from SNe Ia data with CMB anisotropy and galaxy clustering statistics (Tegmark et al. [10]).

For the value of ω to be consistent with the latest observations (Hinshaw et al. [51]; Komatsu et al. [21]), we have the following general condition for $n \neq 0$:

$$t_5 < t < t_6, \tag{78}$$

where

$$t_5 = \frac{1}{k} \left\{ \frac{k^2[m(1.56 - 2r) - 2.88]}{0.39 m\ell_0 r^2} \right\}^{\frac{mr}{2(mr - 2m + 1)}} - \frac{c_0}{k} \tag{79}$$

and

$$t_6 = \frac{1}{k} \left\{ \frac{k^2[m(2.08 - 2r) - 1.84]}{0.52 m\ell_0 r^2} \right\}^{\frac{mr}{2(mr - 2m + 1)}} - \frac{c_0}{k}. \tag{80}$$

For this constraint, we obtain the dark energy EoS to $-1.44 < \omega < -0.92$ which is in good agreement with the limit of the latest observational result in 2009 at 68% confidence level (Hinshaw et al. [51]; Komatsu et al. [21]).

We also observe that if

$$t_0 = \frac{1}{k} \left\{ \frac{4k^2[m(1-r)-r]}{m\ell_0 r^3} \right\}^{\frac{mr}{2(mr-2m+1)}} - \frac{c_0}{k}, \tag{81}$$

then for $t = t_0$, $\omega = -1$ (i.e., cosmological constant dominated universe), and when $t < t_0$, $\omega > -1$ (i.e., quintessence), and for $t > t_0$, $\omega < -1$ (i.e., super quintessence or phantom fluid dominated universe) (Caldwell [49]).

Figure 4, a, b depicts the variations of EoS parameter (ω) with cosmic time t in the two modes of evolution of the universe (i.e., for $q < 0$ and $q > 0$, respectively), as a representative case with appropriate choice of constants of integration and other physical parameters using reasonably well-known situations. From Fig. 4, a, we conclude that in early stage of evolution of the universe, the EoS parameter ω was very small but positive (i.e., the universe was matter-dominated) and at late time it is evolving with negative value (i.e., at the present time). The earlier real matter later on converted to the dark-energy-dominated phase of the universe. In decelerating phase ($q > 0$), the variation of ω with t is clearly shown in Fig. 4, b. From this figure, we observe that ω increases rapidly in the initial stage, it attains maximum value at some epoch closer to the early phase of the universe. In the later stage, it decreases sharply from its maximum value with time to a small negative value and then tends to zero (which may be suitable to describe dusty universe at this moment).

From Eq. (69), we note that energy density of the fluid $\rho(t)$ is a decreasing function of time and $\rho > 0$ under condition

$$t \leqslant \frac{1}{k} \left[\frac{4k^2(m+2)}{mr^2\ell_0} \right]^{\frac{mr}{2(mr-m+1)}} - \frac{c_0}{k}. \tag{82}$$

This behaviour of the energy density $\rho(t)$ is clearly shown in Fig. 5 in the two modes of the evolution of the universe. It is evident that $\rho(t)$ remains positive in both the modes of evolution. However, it decreases more sharply with cosmic time in the decelerating universe compared to accelerating universe.

Using equations (64) and (69), in Eq. (50), the cosmological constant is obtained as

$$\Lambda = \left[\frac{3k^2}{n^2} - \frac{k^2(m+2)}{mr^2} \right] \frac{1}{(kt+c_0)^2} + \frac{1}{4}\ell_0(kt+c_0)^{\frac{2-4m}{mr}}. \tag{83}$$

From Eq. (83), we see that the cosmological term Λ is a decreasing function of time and it is always positive if $\frac{r}{n} > \sqrt{\frac{m+2}{3m}}$. From Fig. 6, a, b, we note this behaviour of cosmological term Λ in the derived DE models in both modes (accelerating and decelerating). We observe that Λ is a decreasing function of
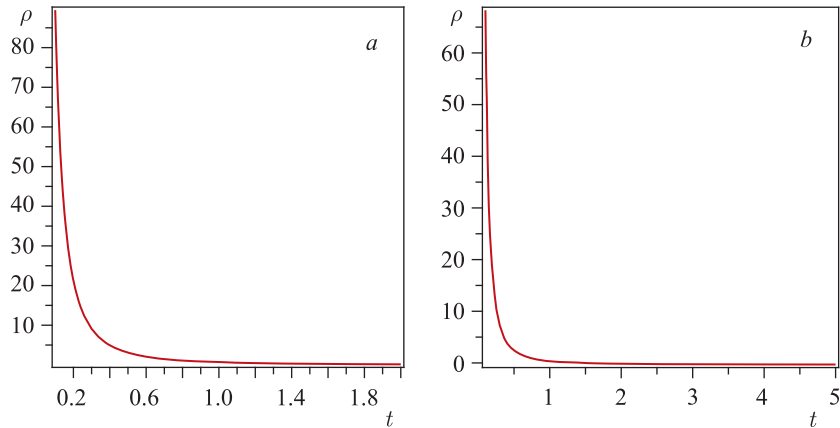
Fig. 5. *a*) The energy density ρ versus t in power-law expansion for $q < 0$. Here $\ell_0 = 1.3$, $r = 2$, $n = 0.5$, $m = 2$, $k = 0.35$. *b*) The energy density ρ versus t in power-law expansion for $q > 0$. Here $\ell_0 = 1.3$, $r = 2.7$, $n = 2$, $m = 0.5$, $k = 1.4$
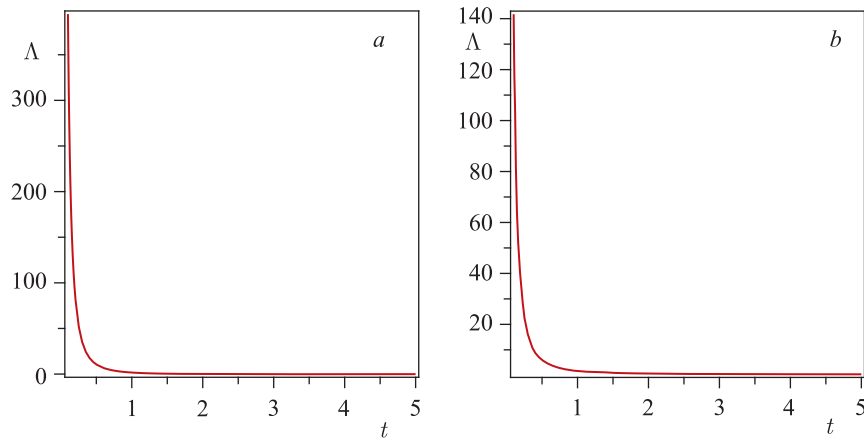
Fig. 6. *a*) The cosmological term Λ versus t in power-law expansion for $q < 0$. Here $\ell_0 = 1.3$, $r = 2$, $n = 0.5$, $m = 2$, $k = 1.4$. *b*) The cosmological term Λ versus t in power-law expansion for $q > 0$. Here $\ell_0 = 1.3$, $r = 2.7$, $n = 2$, $m = 0.5$, $k = 1.4$

time and it approaches a small positive value at present epoch in both the modes. It is remarkable to mention here that DE that explains the observed accelerating expansion of the universe may arise due to the contribution to the vacuum energy of the EoS in a time-dependent background. Thus, our DE model is consistent with the results of recent observations.

2.2. Case (ii): When $n = 0$**, i.e., Model for Exponential Expansion.** After solving the field equations (54)–(56) for the exponential volumetric expansion

(60) by considering Eqs. (58) and (61), we obtain the scale factors as follows:

$$B = \mathit{l}_0 \, e^{\kappa t}, \tag{84}$$

$$A = \mathrm{L}_0 \, e^{m\kappa t}, \tag{85}$$

where l_0 is an integrating constant and $\mathrm{L}_0 = \mathit{l}_0^m$, $\kappa = \dfrac{3D}{2m+1}$.

Thus the Hubble parameter H, scalar of expansion θ, shear scalar σ, and the average anisotropy parameter A_m are given by

$$H = \frac{\kappa(2m+1)}{3}, \tag{86}$$

$$\theta = \kappa(2m+1), \tag{87}$$

$$\sigma^2 = \frac{\kappa^2(m-1)^2}{3}, \tag{88}$$

$$A_m = 2\left(\frac{m-1}{2m+1}\right)^2. \tag{89}$$

Equations (87) and (88) lead to

$$\frac{\sigma^2}{\theta^2} = \frac{1}{3}\left(\frac{m-1}{2m+1}\right)^2. \tag{90}$$

The energy densities of the fluid and deviation-free EoS parameter ω are obtained as

$$\rho = m\kappa^2(m+2) - \frac{1}{4}\ell_1 \, e^{2\kappa(1-2m)t}, \tag{91}$$

$$\omega = \frac{\dfrac{3}{4}\ell_1 \, e^{2\kappa(1-2m)t} - 3(m\kappa)^2}{m\kappa^2(m+2) - \dfrac{1}{4}\ell_1, \, e^{2\kappa(1-2m)t}}, \tag{92}$$

where $\ell_1 = \mathit{l}_0^{2(1-2m)}$.

For the value of ω given by (92) to be consistent with observation (Knop et al. [50]), we have the following general condition:

$$t_1 < t < t_2, \tag{93}$$

where

$$t_1 = \frac{1}{\kappa(1-2m)} \ln\left(\kappa\sqrt{\frac{m(1.23m - 3.34)}{0.3\ell_1}}\right) \tag{94}$$

and

$$t_2 = \frac{1}{\kappa(1-2m)} \ln \left(\kappa \sqrt{\frac{m(2.38m - 1.24)}{0.6\ell_1}} \right). \tag{95}$$

For this constraint, we obtain $-1.67 < \omega < -0.62$, which matches with the limit obtained from observational results coming from SNe Ia data [50].

For the value of EoS parameter ω to be consistent with observation (Tegmark et al. [10]), we have the following general condition:

$$t_3 < t < t_4, \tag{96}$$

where

$$t_3 = \frac{1}{\kappa(1-2m)} \ln \left(\kappa \sqrt{\frac{m(1.67m - 2.66)}{0.41\ell_1}} \right) \tag{97}$$

and

$$t_4 = \frac{1}{\kappa(1-2m)} \ln \left(\kappa \sqrt{\frac{m(2.21m - 1.58)}{0.55\ell_1}} \right). \tag{98}$$

For this constraint, we obtain $-1.33 < \omega < -0.79$, which is in good agreement with the limit obtained from observational results coming from SNe Ia data with CMB anisotropy and galaxy clustering statistics [10].

For the value of ω to be consistent with the latest observations (Hinshaw et al. [51]; Komatsu et al. [21]), we have the following general condition:

$$t_5 < t < t_6, \tag{99}$$

where

$$t_5 = \frac{1}{\kappa(1-2m)} \ln \left(\kappa \sqrt{\frac{m(1.56m - 2.88)}{0.39\ell_1}} \right) \tag{100}$$

and

$$t_6 = \frac{1}{\kappa(1-2m)} \ln \left(\kappa \sqrt{\frac{m(2.08m - 1.84)}{0.52\ell_1}} \right). \tag{101}$$

For this constraint, we obtain the dark energy EoS to $-1.44 < \omega < -0.92$, which matches with the limit of the latest observational result [21, 51].

We also observe that for $t = t_c$, ω vanishes, where t_c is a critical time given by

$$t_c = \frac{1}{\kappa(1-2m)} Ln \left(\frac{2m\kappa}{\sqrt{\ell_1}} \right). \tag{102}$$
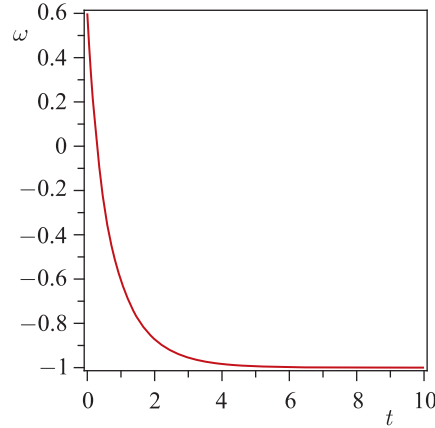
Fig. 7. The EoS parameter ω versus t in exponential-law expansion for $q = -1$. Here $m = 1$, $\kappa = 0.5$, $\ell_1 = 1.3$

We note that the earlier real matter at $t \leqslant t_c$, where $\omega \geqslant 0$, later on at $t > t_c$, where $\omega < 0$ converted to the dark-energy dominated phase of universe which can be seen in Fig. 7.

Also we see that if

$$t_0 = \frac{1}{\kappa(1 - 2m)} Ln\left(2\kappa\sqrt{\frac{m(m-1)}{\ell_1}}\right), \tag{103}$$

then, for $t = t_0$, $\omega = -1$ (i.e., cosmological constant dominated universe), and when $t < t_0$, $\omega > -1$ (i.e., quintessence), and for $t > t_0$, $\omega < -1$ (i.e., super quintessence or phantom fluid dominated universe).

Using Eqs. (86) and (91) in Eq. (50), the cosmological constant in this case is obtained as

$$\Lambda = \frac{1}{4}\ell_1 e^{2\kappa(1-2m)t} + \frac{\kappa^2(m-1)^2}{3}. \tag{104}$$

From Eqs. (91), it is noted that the energy density of the fluid $\rho(t)$ is a decreasing function of time and $\rho(t) > 0$ under condition

$$t \leqslant \frac{1}{\kappa(1 - 2m)} \ln\left[2\kappa\sqrt{\frac{m(m+2)}{\ell_1}}\right]. \tag{105}$$

This behaviour of energy density $\rho(t)$ is shown in Fig. 8.

From Eq. (104), we observe that the cosmological term Λ is a decreasing function of time and it is positive when $m \geqslant 2$. From Fig. 9, we note this behaviour of cosmological term Λ in the derived DE model. Thus, our DE model is consistent with the results of recent observations.
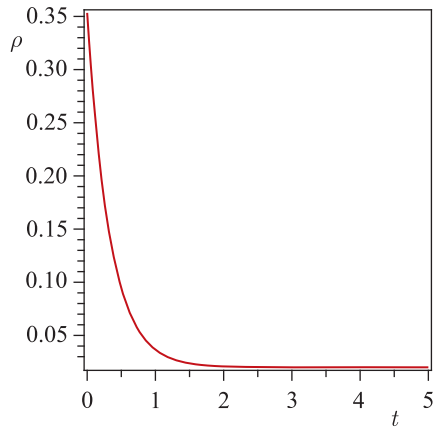
Fig. 8. The energy density ρ versus t in exponential-law expansion for $q = -1$. Here $m = 2$, $\kappa = 0.5$, $\ell_1 = 1.3$
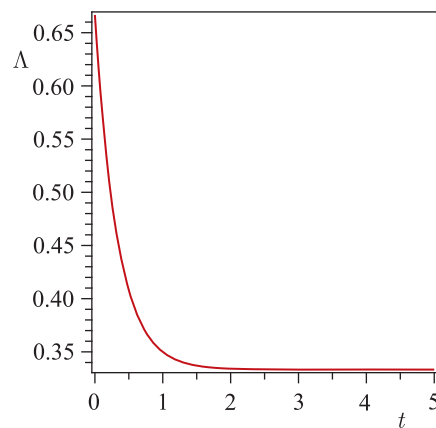
Fig. 9. The cosmological term Λ versus t in exponential-law expansion for $q = -1$. Here $m = 2$, $\kappa = 0.5$, $\ell_1 = 1.3$

The main features of the models are as follows:

• The DE models are based on exact solutions of the Einstein field equations for the anisotropic LRS B-II space-time filled with perfect fluid with variable EoS parameter ω. The exact solutions of the Einstein field equations have been obtained by assuming two different volumetric expansion laws in a way to cover all possible expansions, namely: power-law and exponential-law expansion. The literature has hardly witnessed this sort of exact solutions for the anisotropic LRS B-II space-time. So the derived DE models add one more feather to the literature.

• In both cases (i) and (ii), it is observed that, in early stage, the EoS parameter ω is positive, i.e., the universe was matter dominated in early stage, but in late time, the universe is evolving with negative values, i.e., the present epoch (see, Fig. 4). Thus our DE models represent realistic models.

• In both cases, the DE models present the dynamics of EoS parameter ω provided by Eqs. (70) and (92), respectively, may be accommodated with the acceptable ranges $-1.67 < \omega < -0.62$ of SNe Ia data (Knop et al. [50]), $-1.33 < \omega < -0.79$ (Tegmark et al. [10]) and $-1.44 < \omega < -0.92$ (Hinshaw et al. [51]; Komatsu et al. [21]). It is already observed and shown in previous sections that for different cosmic times, we obtain cosmological constant dominated universe, quintessence and phantom fluid dominated universe (Caldwell [49]), representing the different phases of the universe through out the evolving process. Unlike Robertson–Walker (RW) metric, Bianchi type metrics can admit a DE that wields an anisotropic EoS parameter according to the characteristics. The cosmological data — from the large-scale structures (Tegmark et al. [10]) and

type Ia supernovae (Riess et al. [5]; Astier et al. [136] observations — do not rule out the possibility of an anisotropic DE either (Koivisto and Mota [133]; Mota et al. [134]). Therefore, one cannot rule out the possibility of anisotropic nature of DE at least in the LRS B-II framework.

• Our DE models are of interest because in both the cases the nature of decaying vacuum energy density $\Lambda(t)$ is supported by recent cosmological observations (Garnavich et al. [137, 138]; Perlmutter et al. [2, 3]; Riess et al. [134, 139, 140]; Schmidt et al. [141]). Recent observational data BOOMERanG (de Bernardis et al. [8]), MAXIMA (Hanany et al. [9]) and Sperger [12] reveal the presence of a nonvanishing positive cosmological term Λ.

3. BIANCHI TYPE-III ANISOTROPIC DARK-ENERGY MODELS

We consider the space-time of general Bianchi type-III with the metric

$$ds^2 = -dt^2 + A^2(t)\,dx^2 + B^2(t)\,e^{-2ax}dy^2 + C^2(t)\,dz^2, \qquad (106)$$

where a is the constant.

The solutions of the Einstein field equations are obtained by Pradhan and Amirhashchi [78]. We obtain the expressions for metric coefficient as follows:

$$C = (\ell+1)^{\frac{1}{\ell+1}}\left[\frac{k_1}{\ell\ell_2}t+k_2\right]^{\frac{1}{\ell+1}}, \qquad (107)$$

$$B = \ell_2(\ell+1)^{\frac{\ell}{\ell+1}}\left[\frac{k_1}{\ell\ell_2}t+k_2\right]^{\frac{\ell}{\ell+1}}, \qquad (108)$$

and

$$A = m\ell_2(\ell+1)^{\frac{\ell}{\ell+1}}\left[\frac{k_1}{\ell\ell_2}t+k_2\right]^{\frac{\ell}{\ell+1}}, \qquad (109)$$

respectively, where m, k_1, k_2 are constants of integration and $\ell_2 = \ell_1^{\frac{1}{1-m_1}}m^\ell$, $\ell = \dfrac{m_1}{1-m_1}$.

Hence, the metric (106) reduces to the form

$$ds^2 = -dt^2 + \left[m\ell_2(\ell+1)^{\frac{\ell}{\ell+1}}\left(\frac{k_1}{\ell\ell_2}t+k_2\right)^{\frac{\ell}{\ell+1}}\right]^2 dx^2 +$$

$$+\left[\ell_2(\ell+1)^{\frac{\ell}{\ell+1}}e^{-ax}\left(\frac{k_1}{\ell\ell_2}t+k_2\right)^{\frac{\ell}{\ell+1}}\right]^2 dy^2 + \left[(\ell+1)^{\frac{1}{\ell+1}}\left(\frac{k_1}{\ell\ell_2}t+k_2\right)^{\frac{1}{\ell+1}}\right]^2 dz^2.$$

$$(110)$$

Using the suitable transformation

$$m\ell_2(\ell+1)^{\frac{\ell}{\ell+1}}x = X, \quad \ell_2(\ell+1)^{\frac{\ell}{\ell+1}}y = Y,$$

$$(\ell+1)^{\frac{1}{\ell+1}}z = Z, \quad \frac{k_1}{\ell\ell_2}t + k_2 = T, \tag{111}$$

the metric (110) is reduced to

$$ds^2 = -\beta^2\, dT^2 + T^{2L}dX^2 + T^{2L}\exp\left(-\frac{2a}{N}X\right)dY^2 + T^{\frac{2L}{\ell}}dZ^2, \tag{112}$$

where

$$\beta = \frac{\ell\ell_2}{k_1}, \quad M = (\ell+1)^{\frac{1}{\ell+1}}, \quad N = m\ell_2 M, \quad L = \frac{\ell}{\ell+1}. \tag{113}$$

The expressions for the scalar of expansion θ, average generalized Hubble's parameter, magnitude of shear σ^2, the average anisotropy parameter A_m, deceleration parameter q, and proper volume V for the model (112) are given by

$$\theta = 3H = \frac{(2\ell+1)L}{\ell\beta T}, \tag{114}$$

$$\sigma^2 = \frac{1}{3}\left(\frac{(\ell-1)L}{\ell\beta T}\right)^2, \tag{115}$$

$$A_m = 2\left(\frac{\ell-1}{2\ell+1}\right)^2, \tag{116}$$

$$q = -\frac{\ell\beta}{(2\ell+1)}, \tag{117}$$

$$V = \frac{N^2}{m}M^{\frac{1}{\ell}}T^{\frac{L(2\ell+1)}{\ell}}. \tag{118}$$

The energy density of the fluid, the equation of state parameter ω, and the skewness parameter γ (i.e., deviation from ω along z-axis) are obtained as

$$\rho = \frac{L^2(\ell+2)}{\ell\beta^2 T^2} - \frac{a^2}{N^2 T^{2L}}, \tag{119}$$

$$\omega = \frac{L(\ell^2+\ell+1) - \ell(\ell+1)}{\dfrac{\ell^2 a^2\beta^2}{N^2 L T^{2(L-1)}} - L\ell(\ell+2)}, \tag{120}$$

$$\gamma = \frac{\dfrac{a^2}{N^2 T^{2L}} + \dfrac{L}{\ell^2\beta^2 T^2}[\ell(\ell-1) - L(2\ell^2 - \ell - 1)]}{\dfrac{L^2(\ell+2)}{\ell\beta^2 T^2} - \dfrac{a^2}{N^2 T^{2L}}}. \tag{121}$$

If the present work is compared with experimental results mentioned in B-I, LRS B-II, then one can conclude that the limit of ω provided by Eq. (120) may accommodate with the acceptable range of EoS parameter. Also it is observed that either for $T = 0$ or for $m_1 = 0$, the ω vanishes and our model represents a dusty universe.

For the value of ω to be consistent with observation (Knop et al. [50]), we have the following general condition:

$$T_1 < T < T_2, \tag{122}$$

where

$$T_1 = \left[\frac{0.79\ell a\beta}{N\sqrt{L\{\ell(\ell+1) - L(0.38\ell^2 - 0.24\ell + 1)\}}} \right]^{\frac{1}{(L-1)}} \tag{123}$$

and

$$T_2 = \left[\frac{1.39\ell a\beta}{N\sqrt{L\{\ell(\ell+1) - L(0.67\ell^2 - 2.34\ell + 1)\}}} \right]^{\frac{1}{(L-1)}}. \tag{124}$$

For this constraint, we obtain $-1.67 < \omega < -0.62$, which is in good agreement with the limit obtained from observational results coming from SNe Ia data (Knop et al. [50]). For a special case for which $\ell = 1$, $a = 0.5$, $\beta = 2$, $L = 0.5$, $N = 1$, where $0.899700 < T < 1.153226$, we obtain the same limit $-1.67 < \omega < -0.62$.

From Eq. (120), we have observed that, at cosmic time

$$T = \left[\frac{\ell a\beta}{N\sqrt{L\{L\ell + \ell(\ell+1) - 1\}}} \right]^{\frac{1}{(L-1)}}, \tag{125}$$

$\omega = -1$ (i.e., cosmological constant dominated universe) and when

$$T < \left[\frac{\ell a\beta}{N\sqrt{L\{L\ell + \ell(\ell+1) - 1\}}} \right]^{\frac{1}{(L-1)}}, \tag{126}$$

$\omega > -1$ (i.e., quintessence) and when

$$T > \left[\frac{\ell a\beta}{N\sqrt{L\{L\ell + \ell(\ell+1) - 1\}}} \right]^{\frac{1}{(L-1)}}, \tag{127}$$

$\omega < -1$ (i.e., super quintessence or phantom fluid dominated universe) (Caldwell [49]).

The variation of the EoS parameter ω with cosmic time T is clearly shown in Fig. 10, as a representative case with appropriate choice of constants of integration
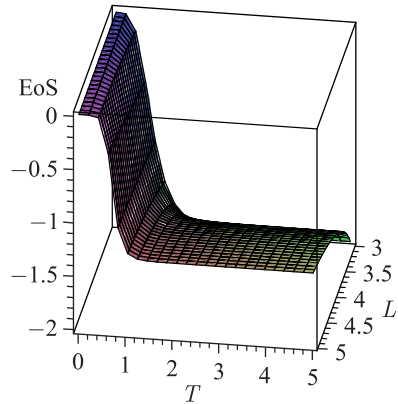
Fig. 10. The plot of the EoS parameter ω versus T and L
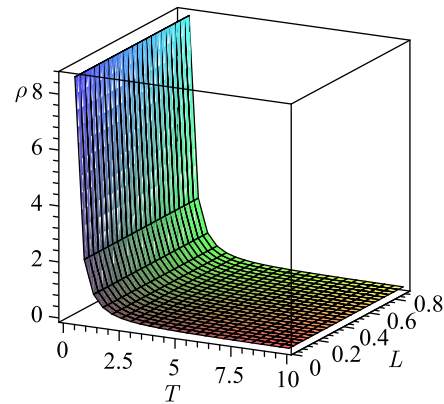
Fig. 11. The plot of the energy density ρ versus T and L

and other physical parameters using reasonably well-known situations. From Fig. 10, we conclude that in early stage of evolution of the universe, the EoS parameter ω was very small but positive (i.e, the universe was matter dominated) and at late time it is evolving with negative value (i.e., at the present time). The earlier real matter later on converted to the dark energy dominated phase of the universe.

From Eq. (119), we note that $\rho(t)$ is a decreasing function of time and $\rho > 0$ for all times. This behaviour is clearly depicted in Fig. 11 as a representative case with appropriate choice of constants of integration and other physical parameters using reasonably well-known situations.

Using equations (114) and (119), in Eq. (50), the cosmological constant is obtained as

$$\Lambda = \frac{L^2(2\ell+1)^2}{3\ell^2\beta^2 T^2} - \frac{L^2(\ell+2)}{\ell\beta^2 T^2} + \frac{a^2}{N^2 T^{2L}}. \tag{128}$$

From Eq. (128), we see that the cosmological term Λ is a decreasing function of time and it approaches a small positive value at late time. From Fig. 12, we note this behaviour of cosmological term Λ in the model. It is remarkable to mention here that the dark energy that explains the observed accelerating expansion of the universe may arise due to the contribution to the vacuum energy of the EoS in a time-dependent background. Thus, our DE model is consistent with the results of recent observations.

From the above results, it can be seen that the spatial volume is zero at $T = 0$ and it increases with the increase of T. This shows that the universe starts evolving with zero volume at $T = 0$ and expands with cosmic time T. In derived model, the energy density tends to infinity at $T = 0$. The model has the

point-type singularity at $T = 0$. The shear scalar diverges at $T = 0$. As $T \to \infty$, the scale factors $A(t)$, $B(t)$, and $C(t)$ tend to infinity. The energy density becomes zero as $T \to \infty$. The expansion scalar and shear scalar all tend to zero as $T \to \infty$. The mean anisotropy parameter is uniform throughout the whole expansion of the universe, when $\ell \neq -1/2$, but for $\ell = -1/2$ it tends to infinity. This shows that the universe is expanding with the increase of cosmic time, but the rate of expansion and shear scalar decrease to zero and tend to isotropic. At the initial stage of expansion, when ρ is large, the Hubble parameter is also large, and with the expansion of the universe H, θ decreases as ρ does. Since $\sigma^2/\theta^2 = \text{const}$ provided

Fig. 12. The plot of the cosmological term Λ versus T and L

$\ell \neq -1/2$, the model does not approach isotropy at any time. The cosmological evolution of Bianchi type-III space-time is expansionary, with all the three scale factors monotonically increasing the function of time. The dynamics of the mean anisotropy parameter depends on the value of ℓ.

From (117), we observe that

$$\text{(i)} \quad \text{for} \quad \ell < -1/2, \quad q > 0,$$

i.e., the model is decelerating and

$$\text{(ii)} \quad \text{for} \quad \ell > -1/2, \quad q < 0,$$

i.e., the model is accelerating. Thus, this case implies an accelerating model of the universe. Recent observations of type Ia supernovae reveal that the present universe is in accelerating phase, and deceleration parameter lies somewhere in the range $-1 < q \leqslant 0$. It follows that our DE model of the universe is consistent with the recent observations.

4. BIANCHI TYPE-V ANISOTROPIC DARK-ENERGY MODELS

We consider the space-time metric of the spatially homogeneous and anisotropic Bianchi type-V of the form

$$ds^2 = -dt^2 + A^2 \, dx^2 + e^{2\alpha x} \left[B^2 \, dy^2 + C^2 \, dz^2 \right], \tag{129}$$

where the metric potentials A, B, and C are functions of cosmic time t alone and α is a constant.
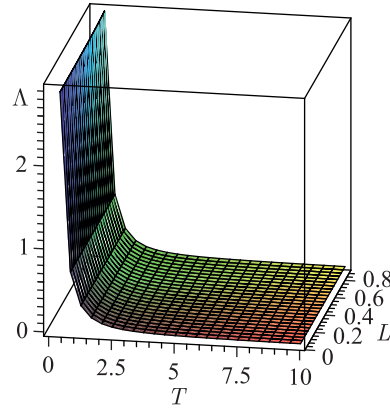
The Einstein field equations (in gravitational units $8\pi G = c = 1$) read as

$$R^i_j - \frac{1}{2}Rg^i_j = -T^{(m)i}_j - T^{(de)i}_j, \tag{130}$$

where $T^{(m)i}_j$ and $T^{(de)i}_j$ are the energy-momentum tensors of perfect fluid and DE, respectively. These are given by

$$\begin{aligned}
T^{(m)i}_j &= \mathrm{diag}\,[-\rho^{(m)}, p^{(m)}, p^{(m)}, p^{(m)}], \\
&= \mathrm{diag}\,[-1, \omega^{(m)}, \omega^{(m)}, \omega^{(m)}]\rho^m,
\end{aligned} \tag{131}$$

and

$$\begin{aligned}
T^{(de)i}_j &= \mathrm{diag}\,[-\rho^{(de)}, p^{(de)}, p^{(de)}, p^{(de)}], \\
&= \mathrm{diag}\,[-1, \omega^{(de)}, \omega^{(de)}, \omega^{(de)}]\rho^{(de)},
\end{aligned} \tag{132}$$

where $\rho^{(m)}$ and $p^{(m)}$ are, respectively, the energy density and pressure of the perfect fluid component or ordinary baryonic matter while $\omega^{(m)} = p^{(m)}/\rho(m)$ is its EoS parameter. Similarly, $\rho^{(de)}$ and $p^{(de)}$ are, respectively, the energy density and pressure of the DE component while $\omega^{(de)} = p^{(de)}/\rho^{(de)}$ is the corresponding EoS parameter. We assume the four-velocity vector $u^i = (1, 0, 0, 0)$ satisfying $u^i u_j = -1$.

In a comoving coordinate system ($u^i = \delta^i_0$), Einstein's field equations (130) with (131) and (132) for B-V metric (129) subsequently lead to the following system of equations:

$$\frac{\ddot{B}}{B} + \frac{\ddot{C}}{C} + \frac{\dot{B}\dot{C}}{BC} - \frac{\alpha^2}{A^2} = -\omega^{(m)}\rho^{(m)} - \omega^{(de)}\rho^{(de)}, \tag{133}$$

$$\frac{\ddot{C}}{C} + \frac{\ddot{A}}{A} + \frac{\dot{C}\dot{A}}{CA} - \frac{\alpha^2}{A^2} = -\omega^{(m)}\rho^{(m)} - \omega^{(de)}\rho^{(de)}, \tag{134}$$

$$\frac{\ddot{A}}{A} + \frac{\ddot{B}}{B} + \frac{\dot{A}\dot{B}}{AB} - \frac{\alpha^2}{A^2} = -\omega^{(m)}\rho^{(m)} - \omega^{(de)}\rho^{(de)}, \tag{135}$$

$$\frac{\dot{A}\dot{B}}{AB} + \frac{\dot{A}\dot{C}}{AC} + \frac{\dot{B}\dot{C}}{BC} - \frac{3\alpha^2}{A^2} = \rho^{(m)} + \rho^{(de)}, \tag{136}$$

$$\frac{2\dot{A}}{A} - \frac{\dot{B}}{B} - \frac{\dot{C}}{C} = 0. \tag{137}$$

The law of energy-conservation equation ($T^{ij}_{;j} = 0$) yields

$$\dot{\rho}^{(m)} + 3(1 + \omega^{(m)})\rho^{(m)}H + \dot{\rho}^{(de)} + 3(1 + \omega^{(de)})\rho^{(de)}H = 0. \tag{138}$$

The Raychaudhuri equation is found to be

$$\dot{\theta} = -\left(1 + 3\omega^{(\mathrm{de})}\right)\rho^{(\mathrm{de})} - \frac{1}{3}\theta^2 - 2\sigma^2. \tag{139}$$

In order to solve the field equations completely, we first assume that the perfect fluid and DE components interact minimally. Therefore, the energy-momentum tensors of the two sources may be conserved separately.

The energy-conservation equation ($T_{;j}^{(m)ij} = 0$) of the perfect fluid gives

$$\dot{\rho}^{(m)} + 3\rho^{(m)}(1 + \omega^{(m)})H = 0, \tag{140}$$

whereas the energy-conservation equation ($T_{;j}^{(\mathrm{de})ij} = 0$) of the DE component leads to

$$\dot{\rho}^{(\mathrm{de})} + 3\rho^{(\mathrm{de})}(\omega^{(\mathrm{de})} + 1)H = 0. \tag{141}$$

Following, Akarsu and Kilinc [73, 74], Yadav [54], and Kumar and Yadav [90], we assume the EoS parameter of the perfect fluid to be constant, that is,

$$\omega^{(m)} = \frac{p^{(m)}}{\rho^{(m)}} = \mathrm{const}, \tag{142}$$

while $\omega^{(\mathrm{de})}$ has been permitted to be a function of time since the current cosmological data from SN Ia, CMB and large scale structures mildly favour dynamically evolving DE crossing the PDL as discussed in the previous section.

Equation (140) can be integrated to obtain

$$\rho^{(m)} = \rho_0 a^{-3(\omega+1)}, \tag{143}$$

where ρ_0 is a positive constant of integration.

Following Saha et al. [142], we take the following *ansatz* for the scale factor, where the increase in term of time evolution is

$$a(t) = \sqrt{t^n\, \mathrm{e}^t}, \tag{144}$$

where n is a positive constant. This *ansatz* generalized the one proposed by Amirhashchi et al. [83]. In literature it is common to use a constant deceleration parameter [73, 74, 85, 90]. The motivation to choose such time-dependent DP is behind the fact that the universe is accelerated expansion at present as observed in recent observations of type Ia supernova [1–6] and CMB anisotropies [7–9] and decelerated expansion in the past. Also, the transition redshift from deceleration expansion to accelerated one is about 0.5. Now for the universe which was decelerating in past and accelerating at the present time, the DP must show signature flipping [143–145]. So, in general, the DP is not a constant but time variable. The motivation to choose such a scale factor (151) yields a time-dependent DP,

$$q = \frac{2n}{(n+t)^2} - 1. \tag{145}$$
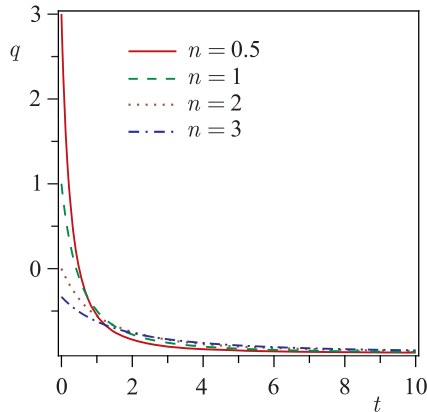
Fig. 13. The deceleration parameter q versus t

From Eq. (145), we observe that $q > 0$ for $t < \sqrt{2n} - n$ and $q < 0$ for $t > \sqrt{2n} - n$. It is observed that for $0 < n < 2$, our model is evolving from deceleration phase to acceleration one. Also, recent observations of SNe Ia expose that the present universe is accelerating and the value of DP lies to some place in the range $-1 < q < 0$. It follows that in our derived model, one can choose the value of DP consistent with the observation. Figure 13 graphs the deceleration parameter (q) versus time which gives the behaviour of q from decelerating to accelerating phase for different values of n.

Using (151), we get the following expressions for scale factors:

$$A(t) = (t^n \, \mathrm{e}^t)^{1/2}, \tag{146}$$

$$B(t) = m(t^n \, \mathrm{e}^t)^{1/2} \exp\left(\ell \int (t^n \, \mathrm{e}^t)^{-3/2} dt\right), \tag{147}$$

$$C(t) = m^{-1}(t^n \, \mathrm{e}^t)^{1/2} \exp\left(-\ell \int (t^n \, \mathrm{e}^t)^{-3/2} dt\right). \tag{148}$$

The expressions for physical parameters such as the Hubble parameter (H), scalar of expansion (θ), shear scalar (σ), spatial volume V, and the anisotropy parameter (A_m) are, respectively, given by

$$\theta = 3H = \frac{3}{2}\left(\frac{n}{t} + 1\right), \tag{149}$$

$$\sigma^2 = \ell^2 \left(t^n \, \mathrm{e}^t\right)^{-3}, \tag{150}$$

$$V = \left(t^n \, \mathrm{e}^t\right)^{3/2} \exp\left(2\alpha x\right), \tag{151}$$

$$A_m = \frac{8\ell^2}{3}\left(\frac{n}{t} + 1\right)^{-2} \left(t^n \, \mathrm{e}^t\right)^{-3}. \tag{152}$$

It is observed that at $t = 0$, the spatial volume vanishes and other parameters θ, σ, H diverge. Hence, the model starts with the Big Bang singularity at $t = 0$. This is a point type singularity since directional scale factors $A(t)$, $B(t)$, and $C(t)$ vanish at initial time.
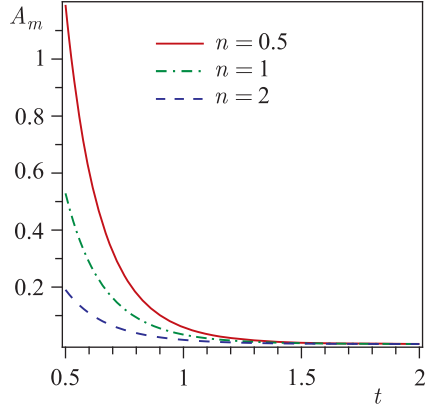
Fig. 14. The anisotropic parameter A_m versus t. Here $\ell = 1$
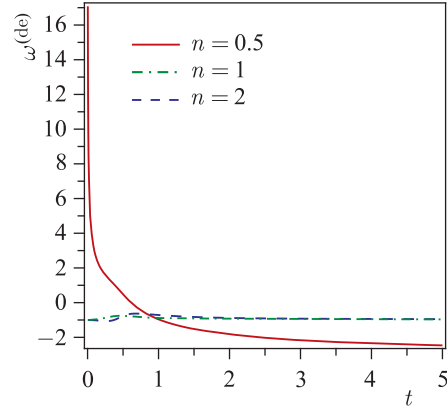
Fig. 15. The DE EoS parameter $\omega^{(\mathrm{de})}$ versus t. Here $\rho_0 = 1$, $\alpha = 1$, $\ell = 1$, $\omega^{(m)} = 0.5$

Figure 14 depicts the variation of anisotropic parameter (A_m) versus cosmic time t. From the figure, we observe that A_m decreases with time and tends to zero as $t \to \infty$ for all values of n. Thus, the observed isotropy of the universe can be achieved in our derived model at present epoch. The shear tensor also tends to zero in this model.

The energy density ($\rho^{(m)}$) of perfect fluid, the pressure ($p^{(\mathrm{de})}$) of DE component, DE density ($\rho^{(\mathrm{de})}$), and the EoS parameter ($\omega^{(\mathrm{de})}$) of DE, for this model, are given by

$$\rho^{(m)} = \rho_0 (t^n \, \mathrm{e}^t)^{-\frac{3}{2}(1+\omega^{(m)})}, \tag{153}$$

$$p^{(\mathrm{de})} = -\frac{3}{4}\left(\frac{n}{t}+1\right)^2 + \frac{n}{t^2} - \ell(t^n \, \mathrm{e}^t)^{-3} + \alpha^2(t^n \, \mathrm{e}^t)^{-1} - \omega^{(m)}\rho_0(t^n \, \mathrm{e}^t)^{-\frac{3}{2}(1+\omega^{(m)})}, \tag{154}$$

$$\rho^{(\mathrm{de})} = -\rho_0(t^n \, \mathrm{e}^t)^{-\frac{3}{2}(1+\omega^{(m)})} + \frac{3}{4}\left(\frac{n}{t}+1\right)^2 + \ell(t^n \, \mathrm{e}^t)^{-3} - 3\alpha^2(t^n \, \mathrm{e}^t)^{-1}, \tag{155}$$

$$\omega^{(\mathrm{de})} =$$
$$= -\frac{\dfrac{3}{4}\left(\dfrac{n}{t}+1\right)^2 - \dfrac{n}{t^2} + \ell(t^n \, \mathrm{e}^t)^{-3} - \alpha^2(t^n \, \mathrm{e}^t)^{-1} + \omega^{(m)}\rho_0(t^n \, \mathrm{e}^t)^{-\frac{3}{2}(1+\omega^{(m)})}}{\dfrac{3}{4}\left(\dfrac{n}{t}+1\right)^2 + \ell(t^n \, \mathrm{e}^t)^{-3} - 3\alpha^2(t^n \, \mathrm{e}^t)^{-1} - \rho_0(t^n \, \mathrm{e}^t)^{-\frac{3}{2}(1+\omega^{(m)})}}. \tag{156}$$

Figure 15 depicts the variation of the DE EoS parameter $\omega^{(\mathrm{de})}$ versus cosmic time t. We observe from the figure that for $n < 1$, $\omega^{(\mathrm{de})}$ varies from nondark

region crossing the PDL ($\omega^{(\mathrm{de})} = -1$) and ultimately approaches the phantom region ($\omega^{(\mathrm{de})} < -1$). But for $n \geqslant 1$, the variation of $\omega^{(\mathrm{de})}$ starts from cosmological constant region ($\omega^{(\mathrm{de})} = -1$) and finally approaches the quintessence region ($\omega^{(\mathrm{de})} > -1$). Therefore, we observe that for $n \geqslant 1$, the variation of $\omega^{(\mathrm{de})}$ in our derived model is consistent with the recent observations of SNe Ia data [50], SNe Ia data with CMBR anisotropy and galaxy clustering statistics [10].

The dark energy with $\omega^{(\mathrm{de})} < -1$, the phantom component of the universe, leads to uncommon cosmological scenarios as it was pointed out by Caldwell et al. [146]. First of all, there is a violation of the dominant energy condition (DEC), since $\rho + p < 0$. The energy density grows up to infinity in a finite time, which leads to a big rip, characterized by a scale factor blowing up in this finite time. These sudden future singularities are, nevertheless, not necessarily produced by a fluid violating DEC. Cosmological solutions for phantom matter which violate the weak energy condition were found by Dabrowski et al. [147]. Caldwell [49], Srivastava [40], Yadav [54] have investigated phantom models with $\omega^{(\mathrm{de})} < -1$ and also suggested that at late time, phantom energy has appeared as a potential DE candidate which violets the weak as well as strong energy condition.

The left-hand sides of energy conditions have been depicted in Figs. 16 and 17 for different values of n. From Fig. 16, for $n = 0.5$ (i.e., phantom model) (see, Fig. 13), we observe that

(i) $\rho^{(\mathrm{de})} \geqslant 0$,   (ii) $\rho^{(\mathrm{de})} + p^{(\mathrm{de})} \leqslant 0$,   (iii) $\rho^{(\mathrm{de})} + 3p^{(\mathrm{de})} < 0$.

Thus, from the above expressions, we observe that the phantom model violates both the strong and weak energy conditions, as expected.
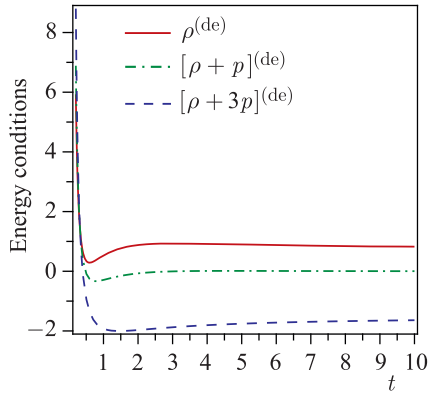
Fig. 16. Energy conditions versus t for $n = 0.5$. Here $\rho_0 = 1$, $\ell = \alpha = 1$, $\omega^{(m)} = 0.5$
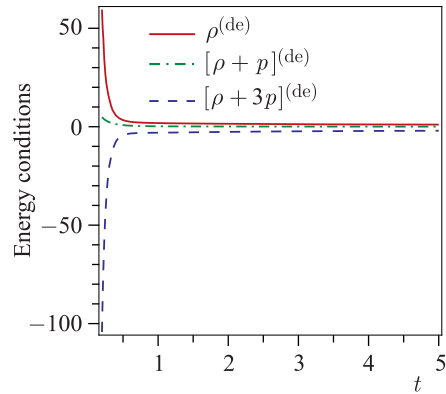
Fig. 17. Energy conditions versus t for $n = 1$. Here $\rho_0 = 1$, $\ell = \alpha = 1$, $\omega^{(m)} = 0.5$

Further, from Fig. 17, for $n \geqslant 1$ (i.e., quintessence model) (see Fig. 13), we observe that

(i) $\rho^{(\mathrm{de})} \geqslant 0$,   (ii) $\rho^{(\mathrm{de})} + p^{(\mathrm{de})} \geqslant 0$,   (iii) $\rho^{(\mathrm{de})} + 3p^{(\mathrm{de})} < 0$.

Thus, the quintessence model violates the strong energy condition as the same is predicted by current astronomical observations.

The perfect fluid density parameter ($\Omega^{(m)}$) and DE density parameter ($\Omega^{(\mathrm{de})}$) are given by

$$\Omega^{(m)} = \frac{4}{3}\rho_0 \left(\frac{n}{t} + 1\right)^2 (t^n \, \mathrm{e}^t)^{-\frac{3}{2}(1+\omega^{(m)})}, \tag{157}$$

$$\Omega^{(\mathrm{de})} = 1 + \frac{4}{3} \left(\frac{n}{t} + 1\right)^{-2} \left[-\rho_0 (t^n \, \mathrm{e}^t)^{-\frac{3}{2}(1+\omega^{(m)})} + \ell^2 (t^n \, \mathrm{e}^t)^{-3} - 3\alpha (t^n \, \mathrm{e}^t)^{-1} \right]. \tag{158}$$

Thus the overall density parameter (Ω) is obtained as

$$\Omega = \Omega^{(m)} + \Omega^{(\mathrm{de})} = 1 + \ell^2 (t^n \, \mathrm{e}^t)^{-3} - 3\alpha (t^n \, \mathrm{e}^t)^{-1}. \tag{159}$$

Figure 18 depicts the variation of the density parameter (Ω) versus cosmic time t for different values of n during the evolution of the universe. From Fig. 18, it can be seen that the total energy density Ω tends to 1 for sufficiently large time which is supported by the current observations [148–151].

A convenient method to describe models close to Λ CDM is based on the cosmic jerk parameter j, a dimensionless third derivative of the scale factor with respect to the cosmic time [152–156]. A deceleration-to-acceleration transition occurs for models with a positive value of j_0 and negative q_0. Flat Λ CDM models have a constant jerk $j = 1$. The jerk parameter in cosmology is defined as the dimensionless third derivative of the scale factor with respect to cosmic time

Fig. 18. The total energy density parameter Ω versus t. Here $\alpha = \ell = 1$

$$j(t) = \frac{1}{H^3} \frac{\dddot{a}}{a} \tag{160}$$

and in terms of the scale factor to cosmic time

$$j(t) = \frac{(a^2 H^2)''}{2H^2}, \tag{161}$$

where the "dots" and "primes" denote derivatives with respect to cosmic time and scale factor, respectively. One can rewrite Eq. (160) as

$$j(t) = q + 2q^2 - \frac{\dot{q}}{H}.\qquad(162)$$

Equations (145) and (162) reduce to

$$j(t) = 1 - \frac{6n}{(n+t)^2} + \frac{8n}{(n+1)^3}.\qquad(163)$$

This value overlaps with the value $j \simeq 2.16$ obtained from the combination of three kinematical data sets: the gold sample of type Ia supernovae [5], the SNIa data from the SNLS project [136], and the X-ray galaxy cluster distance measurements [157] for

$$t = 3.45 \cdot 10^{-2} A - \frac{50n}{A} - n,\qquad(164)$$

where $A = 10^4 n[8.41 + 1.45\sqrt{(14.4n + 33.6)}]^{1/3}$.

In this section, we have studied a spatially homogeneous and anisotropic Bianchi type-V space-time filled with perfect fluid and anisotropic DE possessing dynamic energy density. The field equations have been solved exactly with suitable physical assumptions. The solutions satisfy the energy conservation Eq. (138) and the Raychaudhuri Eq. (139) identically. Therefore, exact and physically viable Bianchi type-V model has been obtained.

The main features of the model are as follows:

• For different values of n, the anisotropic parameter A_m tends to zero for sufficiently large time. Hence, the present model is isotropic at late time which is consistent with the current observations.

• The present DE model has a transition of the universe from the early deceleration phase to the recent acceleration phase (see Fig. 13), which is in good agreement with recent observations [17].

• In the present study, we find that for $n \geqslant 1$, the quintessence model is consistent with the present and expected future evolution of the universe. The quintessence model approaches to isotropy at late time (see Figs. 13 and 15). For other models (for $n < 1$), we observe the phantom scenario.

• The derived phantom model violates both the strong and weak energy conditions, whereas the quintessence model violates only the strong energy condition (see Figs. 16 and 17).

• The total density parameter (Ω) approaches 1 for sufficiently large time (see Fig. 18), which is reproducible with current observations [148–151].

• The cosmic jerk parameter in our descended model is also found to be in good agreement with the recent data of astrophysical observations, namely the

gold sample of type Ia supernovae [5], the SNIa data from the SNLS project [136], and the X-ray galaxy cluster distance measurements [17].

• Our special choice of scale factor yields a time-dependent deceleration parameter which represents a model of the universe which evolves from decelerating phase to an accelerating phase, whereas in Yadav [54], Kumar and Yadav [90] only the evolution takes place either in an accelerating or a decelerating phase.

• For different choice of n, we can generate a class of DE models in Bianchi type-V space-time. It is observed that such DE models are also in good harmony with current observations. Thus, the solutions demonstrated in this paper may be useful for better understanding of the characteristic of anisotropic DE in the evolution of the universe within the framework of Bianchi type-V space-time.

5. BIANCHI TYPE-VI$_0$ ANISOTROPIC DARK-ENERGY MODELS

We consider totally anisotropic Bianchi type-VI$_0$ line element, given by

$$ds^2 = -dt^2 + A^2\,dx^2 + B^2\,\mathrm{e}^{2x}\,dy^2 + C^2\,\mathrm{e}^{-2x}\,dz^2, \tag{165}$$

where the metric potentials A, B, and C are functions of t alone. This ensures that the model is spatially homogeneous.

In a comoving co-ordinate system, Einstein's field equations (4) for B-VI$_0$ metric (165) subsequently lead to the following system of equations:

$$\frac{\ddot{B}}{B} + \frac{\ddot{C}}{C} + \frac{\dot{B}\dot{C}}{BC} + \frac{1}{A^2} = -\omega\rho, \tag{166}$$

$$\frac{\ddot{C}}{C} + \frac{\ddot{A}}{A} + \frac{\dot{C}\dot{A}}{CA} - \frac{1}{A^2} = -(\omega + \delta)\rho, \tag{167}$$

$$\frac{\ddot{A}}{A} + \frac{\ddot{B}}{B} + \frac{\dot{A}\dot{B}}{AB} - \frac{1}{A^2} = -(\omega + \gamma)\rho, \tag{168}$$

$$\frac{\dot{A}\dot{B}}{AB} + \frac{\dot{B}\dot{C}}{BC} + \frac{\dot{C}\dot{A}}{CA} - \frac{1}{A^2} = \rho, \tag{169}$$

$$\frac{\dot{C}}{C} - \frac{\dot{B}}{B} = 0. \tag{170}$$

Here and in what follows an over dot denotes ordinary differentiation with respect to t.

By considering constant deceleration parameter, Amirhashchi et al. [86] obtained the solutions of field Eqs. (166)–(170) as metric functions as follows:

$$B(t) = \ell_1(kt + c_1)^{\frac{1}{mr}}, \tag{171}$$

$$C(t) = \ell_2(kt + c_1)^{\frac{1}{mr}}, \tag{172}$$

$$A(t) = \ell_3(kt + c_1)^{\frac{1}{r}}, \tag{173}$$

where, c_3 is an integrating constant and $\ell_1 = c_3^{\frac{3}{n(m+2)}}$, $\ell_2 = \ell\ell_1$, $\ell_3 = \ell_1^m$, and $r = \frac{n(m+2)}{3m}$.

Hence, the model (165) reduces to

$$ds^2 = -dt^2 + \ell_3^2(kt + c_1)^{\frac{2}{r}}dx^2 + \ell_1^2(kt + c_1)^{\frac{2}{mr}}e^{2x}dy^2 + \ell_2^2(kt + c_1)^{\frac{2}{mr}}e^{-2x}dz^2. \tag{174}$$

The expressions for the Hubble parameter H, scalar of expansion θ, shear scalar σ, and the average anisotropy parameter A_m for model (174) are given by

$$\theta = 3H = \frac{3k}{n(kt + c_1)}, \tag{175}$$

$$\sigma^2 = \frac{1}{3}\left[\frac{k(m-1)}{mr}\right]^2 \frac{1}{(kt + c_1)^2}, \tag{176}$$

$$A_m = \frac{n[n(m^2 + 2) - 2mr(m + 2)]}{3m^2r^2} + 1. \tag{177}$$

The energy density of the fluid, the EoS parameter ω, and skewness parameters δ (or γ) (i.e., deviations from ω along y-axis and z-axis) are computed as

$$\rho = \frac{k^2(2m + 1)}{m^2r^2}(kt + c_1)^{-2} - \ell_0(kt + c_1)^{-\frac{2}{r}}, \tag{178}$$

where $\ell_0 = 1/\ell_3^2$,

$$\omega = \frac{\frac{k^2(1 - 2mr)}{m^2r^2}(kt + c_1)^{-2} + \ell_0(kt + c_1)^{-\frac{2}{r}}}{\ell_0(kt + c_1)^{-\frac{2}{r}} - \frac{k^2(2m + 1)}{m^2r^2}(kt + c_1)^{-2}}. \tag{179}$$

$$\delta = \gamma = \frac{\frac{k^2\{m[(m + 1) - r(m - 1)] - 2\}}{m^2r^2}(kt + c_1)^{-2} - 2\ell_0(kt + c_1)^{-\frac{2}{r}}}{\ell_0(kt + c_1)^{-\frac{2}{r}} - \frac{k^2(2m + 1)}{m^2r^2}(kt + c_1)^{-2}}. \tag{180}$$

From Eq. (179), it is observed that the equation-of-state parameter ω is time-dependent, it can be a function of redshift z or scale factor a as well.

If the present work is compared with experimental results (Knop et al. [50]; Tegmark et al. [10]; Hinshaw et al. [51]; Komatsu et al. [21]), then one can conclude that the limit of ω provided by equation (179) may be accommodated with the acceptable range of EoS parameter. Also it is observed that at $t = t_c$, ω vanishes, where t_c is a critical time given by

$$t_c = \frac{1}{k} \left(\frac{mr}{k} \sqrt{\frac{\ell_0}{2mr - 1}} \right)^{\frac{r}{1-r}} - \frac{c_1}{k}. \tag{181}$$

Thus, for this particular time, our model represents a dusty universe. We also note that the earlier real matter at $t \leqslant t_c$, where $\omega \geqslant 0$, later on at $t > t_c$, where $\omega < 0$, is converted to the dark-energy dominated phase of universe.

For the value of ω to be consistent with observation (Knop et al. [50]), we have the following general condition:

$$t_1 < t < t_2, \tag{182}$$

where

$$t_1 = \frac{1}{k} \left(\frac{k}{mr} \sqrt{\frac{m(2r + 3.34) + 0.67}{2.67\ell_0}} \right)^{\frac{r}{r-1}} - \frac{c_1}{k} \tag{183}$$

and

$$t_2 = \frac{1}{k} \left(\frac{k}{mr} \sqrt{\frac{m(2r + 1.24) - 0.38}{1.62\ell_0}} \right)^{\frac{r}{r-1}} - \frac{c_1}{k}. \tag{184}$$

For this constraint, we obtain $-1.67 < \omega < -0.62$ which is in good agreement with the limit obtained from observational results coming from SNe Ia data [50].

For the value of ω to be consistent with observation (Tegmark et al. [10]), we have the following general condition:

$$t_3 < t < t_4, \tag{185}$$

where

$$t_3 = \frac{1}{k} \left(\frac{k}{mr} \sqrt{\frac{m(2r + 2.66) + 0.33}{2.33\ell_0}} \right)^{\frac{r}{r-1}} - \frac{c_1}{k} \tag{186}$$

and

$$t_4 = \frac{1}{k} \left(\frac{k}{mr} \sqrt{\frac{m(2r + 1.58) - 0.21}{1.79\ell_0}} \right)^{\frac{r}{r-1}} - \frac{c_1}{k}. \tag{187}$$

For this constraint, we obtain $-1.33 < \omega < -0.79$ which is in good agreement with the limit obtained from observational results coming from SNe Ia data with CMB anisotropy and galaxy clustering statistics [10].

For the value of ω to be consistent with the latest observations (Hinshaw et al. [51]; Komatsu et al. [21]), we have the following general condition:

$$t_5 < t < t_6, \tag{188}$$

where

$$t_5 = \frac{1}{k} \left(\frac{k}{mr} \sqrt{\frac{m(2r + 2.88) + 0.44}{2.44\ell_0}} \right)^{\frac{r}{r-1}} - \frac{c_1}{k} \tag{189}$$

and

$$t_6 = \frac{1}{k} \left(\frac{k}{mr} \sqrt{\frac{m(2r + 1.84) - 0.08}{1.92\ell_0}} \right)^{\frac{r}{r-1}} - \frac{c_1}{k}. \tag{190}$$

For this constraint, we obtain the dark-energy EoS to $-1.44 < \omega < -0.92$ which is in good agreement with the limit of the latest observational result [21,51].

We also observe that if

$$t_0 = \frac{1}{k} \left[\frac{k}{r} \sqrt{\frac{r+1}{m\ell_0}} \right]^{\frac{r}{r-1}} - \frac{c_1}{k}, \tag{191}$$

then for $t = t_0$, $\omega = -1$ (i.e., cosmological constant dominated universe), and when $t < t_0$, $\omega > -1$ (i.e., quintessence), and for $t > t_0$, $\omega < -1$ (i.e., super quintessence or phantom fluid dominated universe) (Caldwell [49]).

Figures 19 and 20 depict the variation of EOS parameter (ω) versus cosmic time (t) in the two modes (i.e., $q < 0$ and $q > 0$) of evolution of the universe, as a representative case with appropriate choice of constants of integration and other physical parameters using reasonably well-known situations. From Figs. 19 and 20, we observe that in early stage of evolution of the universe, the EoS parameter ω was positive (i.e., the universe was matter-dominated) and at late time, it is evolving with negative value (i.e., at the present epoch). The earlier real matter later on is converted to the dark-energy dominated phase of the universe in both accelerating and decelerating modes.

From Eq. (178), we note that energy density of the fluid $\rho(t)$ is a decreasing function of time and $\rho \geqslant 0$, when

$$t \leqslant \frac{1}{k} \left[\frac{k}{mr} \sqrt{\frac{2m+1}{\ell_0}} \right]^{\frac{r}{r-1}} - \frac{c_1}{k}. \tag{192}$$

Figures 21 and 22 are plots of energy density of the fluid (ρ) versus time in accelerating and decelerating modes of the universe, respectively. Here we observe that ρ is a positive decreasing function of time and it approaches zero as $t \to \infty$.
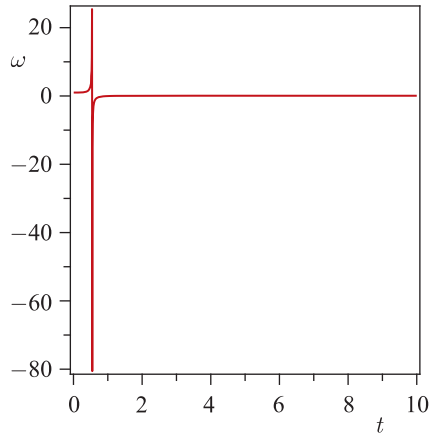
Fig. 19. The EoS parameter ω versus t in power-law expansion for $q < 0$. Here $n = 0.5$, $m = 2$, $r = 0.33$, $k = 1$, $\ell_0 = 1$
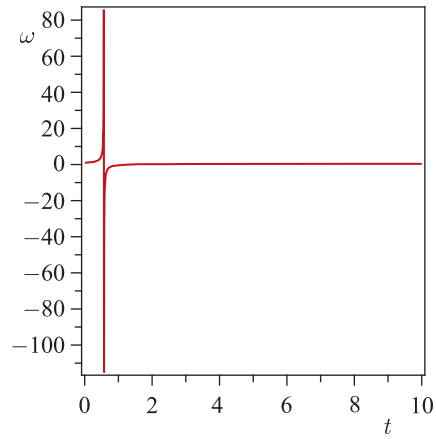
Fig. 20. The EoS parameter ω versus t in power-law expansion for $q > 0$. Here $n = 1.2$, $m = 3$, $r = 0.66$, $k = 1$, $\ell_0 = 1$
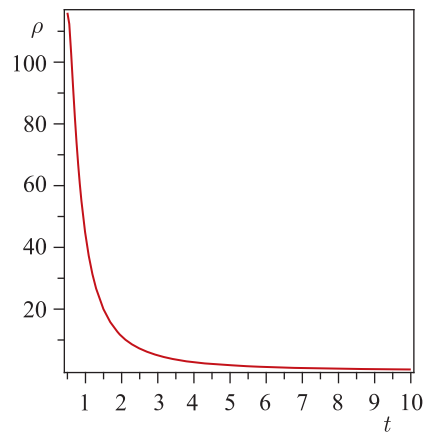
Fig. 21. The energy density ρ versus t in power-law expansion for $q < 0$. Here $n = 0.5$, $m = 2$, $r = 0.33$, $k = 1$, $\ell_0 = 1$
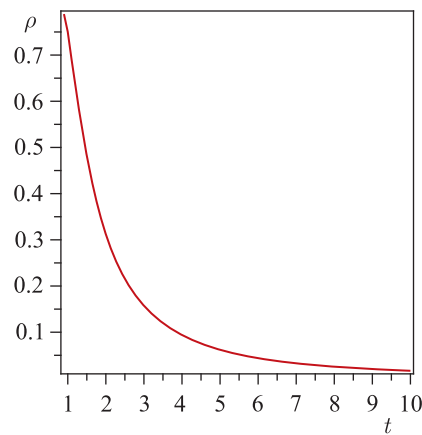
Fig. 22. The energy density ρ versus t in power-law expansion for $q > 0$. Here $n = 1.2$, $m = 3$, $r = 0.66$, $k = 1$, $\ell_0 = 1$

Using Eqs. (175) and (178) in Eq. (50), the cosmological constant is obtained as

$$\Lambda = \left[\frac{3k^2}{n^2} - \frac{k^2(2m+1)}{m^2r^2} \right] (kt + c_1)^{-2} + \ell_0(kt + c_1)^{-\frac{2}{r}}. \qquad (193)$$
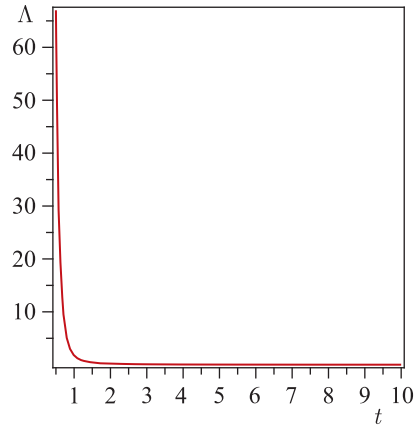
Fig. 23. The cosmological constant Λ versus t in power-law expansion for $q < 0$. Here $n = 0.5$, $m = 2$, $r = 0.33$, $k = 1$, $\ell_0 = 1$
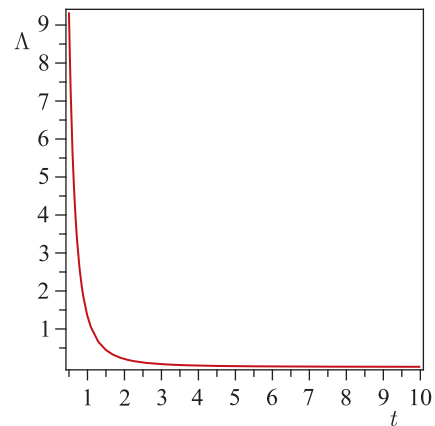
Fig. 24. The cosmological constant Λ versus t in power-law expansion for $q > 0$. Here $n = 1.2$, $m = 3$, $r = 0.66$, $k = 1$, $\ell_0 = 1$

From Eq. (193), we observe that Λ is a decreasing function of time and it is always positive when

$$t > \left[\frac{1}{\ell_0} \left(\frac{k^2(2m+1)}{m^2 r^2} - \frac{3k^2}{n^2} \right) \right]^{\frac{r}{2(r-1)}} - \frac{c_1}{k}. \tag{194}$$

Figures 23 and 24 are plots of cosmological constant Λ versus time in accelerating and decelerating modes of the universe, respectively. In both modes, we observe that cosmological parameter is a decreasing function of time and it approaches a small positive value at late time (i.e., at present epoch). Recent cosmological observations [1–5] suggest the existence of a positive cosmological constant Λ with the magnitude $\Lambda(G\hbar/c^3) \approx 10^{-123}$. These observations on magnitude and redshift of type Ia supernova suggest that our universe may be an accelerating one with induced cosmological density through the cosmological Λ-term. Thus, the nature of Λ in our derived DE model is supported by recent observations.

It can be seen that all the kinematical parameters H, θ, and σ diverge at the initial singularity. There is a point type singularity (MacCallum [132]) at $t = -c_1/k$ in the model. The mean anisotropic parameter is constant and it increases as n increases. Thus, the dynamics of the mean anisotropy parameter depends on the value of n. Since $\sigma^2/\theta^2 = \text{const}$, the model does not approach isotropy through the whole evolution of the universe.

To find different solution of the previous field equations (166)–(170), we take the following *ansatz* for the scale factor, where increase in term of time

evolution is

$$a(t) = \sqrt{t^n \, e^t},\tag{195}$$

where n is a positive constant. Pradhan and Amirhashchi [79] and Saha et al. [142] have examined the relation (195) in studying two-fluid scenario for dark-energy models in an FRW universe and accelerating DE models in Bianchi type-V space-times, respectively. This *ansatz* generalized the one proposed by Amirhashchi et al. [83]. If we put $n = 0$ in Eq. (195), it is reduced to $a(t) = \sqrt{e^t}$, i.e., an exponential law of variation of scale factor. This choice of scale factor yields a time-dependent deceleration parameter (see Eq. (201)) such that before DE era, the corresponding solution gives inflation and radiation/matter dominance era with subsequent transition from deceleration to acceleration. Thus, our choice of scale factor is physically acceptable.

It is worth to mention here that one can also select many-to-many *ansatz* other than Eq. (195) which mimics accelerating universe but one should also be careful to check the physical acceptability and stability of their corresponding solutions, otherwise one does not prove any relation of such solutions with observable universe. Equation (195) yields physically plausible solutions.

In this case, we obtain the expressions for metric functions as follows:

$$B(t) = \ell_1 (t^n \, e^t)^{\frac{3}{2(m+2)}},\tag{196}$$

$$C(t) = \ell_2 (t^n \, e^t)^{\frac{3}{2(m+2)}},\tag{197}$$

$$A(t) = \ell_3 (t^n \, e^t)^{\frac{3m}{2(m+2)}},\tag{198}$$

where, $\ell_1 = k^{-\frac{1}{(m+2)}}$, $\ell_2 = \ell \ell_1$, $\ell_3 = \ell_1^m$, and k is an integrating constant.

Hence, the model (165) reduces to

$$ds^2 = -dt^2 + \ell_3^2 (t^n \, e^t)^{\frac{6m}{(m+2)}} dx^2 + \ell_1^2 (t^n \, e^t)^{\frac{6}{(m+2)}} dy^2 + \ell_2^2 (t^n \, e^t)^{\frac{6}{(m+2)}} dz^2.\tag{199}$$

The expressions for the Hubble parameter (H), scalar of expansion (θ), shear scalar (σ), the spatial volume (V), and the average anisotropy parameter (A_m) for the model (199) are given by

$$\theta = 3H = \frac{3}{2}\left(1 + \frac{n}{t}\right),\tag{200}$$

$$q = \frac{2n}{(n+t)^2} - 1,\tag{201}$$

$$\sigma^2 = \frac{3}{4}\left(\frac{m-1}{m+2}\right)^2 \left(1 + \frac{n}{t}\right)^2,\tag{202}$$

$$V = (t^n \, e^t)^{3/2},\tag{203}$$

$$A_m = 2 \left(\frac{m-1}{m+2} \right)^2 . \tag{204}$$

From Eqs. (200)–(204), it is observed that at $t = 0$, the spatial volume vanishes and other parameters θ, σ, H diverge. Hence the model starts with the Big Bang singularity at $t = 0$. This is a point type singularity [27] since directional scale factors $A(t)$, $B(t)$, and $C(t)$ vanish at initial time. Since $\sigma^2/\theta^2 \neq 0$ except $m = 1$, hence the model is anisotropic for all values of m except for $m \neq 1$. The dynamics of the mean anisotropy parameter depends on the value of m. We observe that when $m = 1$, $A_m = 0$ (i.e., the case of isotropy). Thus, the observed isotropy of the model can be achieved in cosmological constant region (see Fig. 26).

The energy density of the fluid, the EoS parameter ω, and the skewness parameters δ (or γ) (i.e., deviations from ω along y-axis and z-axis) are computed as

$$\rho = \frac{9}{4} \left(\frac{2m+1}{m+2} \right) \left(1 + \frac{n}{t} \right)^2 - \ell_0 (t^n \, \mathrm{e}^t)^{-\frac{3m}{(m+2)}}, \tag{205}$$

$$\omega = \frac{\dfrac{27}{4(m+2)^2} \left(1 + \dfrac{n}{t} \right)^2 - \dfrac{3n}{(m+2)t^2} + \ell_0 (t^n \, \mathrm{e}^t)^{-\frac{3m}{(m+2)}}}{\ell_0 (t^n \, \mathrm{e}^t)^{-\frac{3m}{(m+2)}} + \dfrac{9}{4} \left(\dfrac{2m+1}{m+2} \right) \left(1 + \dfrac{n}{t} \right)^2}, \tag{206}$$

$$\delta = \gamma = \frac{\dfrac{3}{4} \left(\dfrac{m-1}{m+2} \right) \left\{ \left(1 + \dfrac{n}{t} \right)^2 - \dfrac{2n}{t^2} \right\} - 2\ell_0 (t^n \, \mathrm{e}^t)^{-\frac{3m}{(m+2)}}}{\ell_0 (t^n \, \mathrm{e}^t)^{-\frac{3m}{(m+2)}} - \dfrac{9}{4} \left(\dfrac{2m+1}{m+2} \right) \left(1 + \dfrac{n}{t} \right)^2}, \tag{207}$$

where $\ell_0 = 1/\ell_3^2$.

From Eq. (206), it is observed that the equation-of-state parameter ω is time-dependent, it can be a function of redshift z or scale factor a as well (as already discussed in Introduction).

So, if the present work is compared with experimental results [10, 21, 50, 51], then one can conclude that the limit of ω provided by Eq. (206) may be accommodated with the acceptable range of EoS parameter. Also it is observed that at $t = t_c$, ω vanishes, where t_c is a critical time given by the following relation:

$$\frac{27}{4(m+2)^2} \left(1 + \frac{n}{t_c} \right)^2 - \frac{3n}{(m+2)t_c^2} + \ell_0 (t_c^n \, \mathrm{e}^{t_c})^{-\frac{3m}{(m+2)}} . \tag{208}$$

Thus, for this particular time, our model represents a dusty universe. We also note that the earlier real matter at $t \leqslant t_c$, where $\omega \geqslant 0$, later on at $t > t_c$, where $\omega < 0$, is converted to the dark-energy dominated phase of universe.
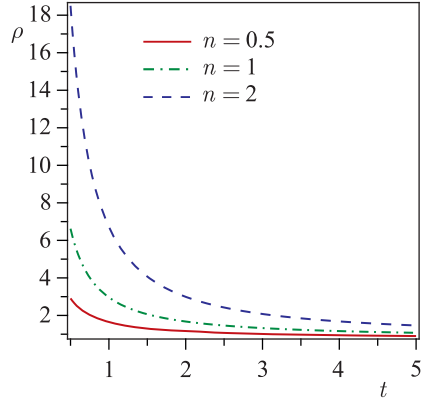
Fig. 25. The energy density ρ versus t. Here $\ell_0 = 0.1$, $m = 1$
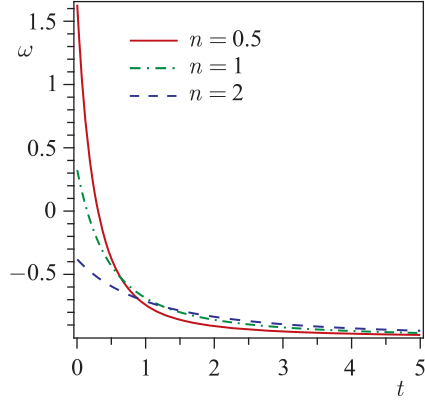
Fig. 26. The plot of the EoS parameter ω versus t. Here $\ell_0 = 0.1$, $m = 1$

From Eq. (205), we note that energy density of the fluid $\rho(t)$ is a decreasing function of time and $\rho \geqslant 0$ when

$$\left(1 + \frac{n}{t}\right)^2 (t^n \, e^t)^{\frac{3m}{(m+2)}} \geqslant \frac{4\ell_0}{9}\left(\frac{m+2}{2m+1}\right).\tag{209}$$

Figure 25 is the plot of energy density of the fluid (ρ) versus time in accelerating mode of the universe. Here we observe that ρ is a positive decreasing function of time and it approaches zero as $t \to \infty$.

Figure 26 depicts the variation of EoS parameter (ω) versus cosmic time (t) in evolution of the universe, as a representative case with appropriate choice of constants of integration and other physical parameters using reasonably well-known situations. For $m = 1$, we obtain isotropic model which is studied here as a representative case. From Fig. 26, we observed that at the initial time there is quintessence ($\omega > -1$) region and at late time it approaches the cosmological constant ($\omega = -1$) scenario. This is a situation in the early universe where quintessence dominated universe (Caldwell [49]) may be playing an important role for EoS parameter. Since ω approaches -1 for sufficiently large time, so its value is consistent with the range of all of the three observations [10, 21, 50, 51].

Using Eqs. (201) and (205) in Eq. (50), the expression for cosmological constant is obtained as

$$\Lambda = -\frac{3}{4}\left(\frac{5m+1}{m+2}\right)\left(1 + \frac{n}{t}\right)^2 + \ell_0(t^n \, e^t)^{-\frac{3m}{(m+2)}}.\tag{210}$$

From Eq. (210), we observe that Λ is a decreasing function of time and it is

always positive when

$$\left(1 + \frac{n}{t}\right)^2 (t^n\, \mathrm{e}^t)^{\frac{3m}{(m+2)}} < \frac{4\ell_0}{3}\left(\frac{m+2}{5m+1}\right). \qquad (211)$$

In general relativity, the Bianchi identities for the Einstein tensor G_{ij} and the vanishing covariant divergence of the energy-momentum tensor T_{ij}, together imply that the cosmological Λ term is constant. In theories with a variable Λ-term, one either introduces new terms (involving scalar fields, for instance) into the left-hand side of the Einstein field equations to cancel the nonzero divergence of Λg_{ij} (Bergmann [158]; Wagoner [159]), or interprets Λ as a matter source and moves it to the right-hand side of the field equations (Zeldovich [160]), in which case energy-momentum conservation is understood to mean $T^{*ij}_{;j} = 0$, where $T^*_{ij} = T_{ij} - (\Lambda/8\pi G)g_{ij}$. Here it means that the first assumption that leads to the cosmological constant problem is made, and the vacuum has a nonzero energy density. If such a vacuum energy density exists, the Lorentz invariance requires that it has the form $\langle T_{\mu\nu}\rangle = -\langle\rho\rangle g_{\mu\nu}$. This allows one to define an effective cosmological constant and a total effective vacuum energy density $\Lambda_{\mathrm{eff}} = \Lambda + 8\pi G\langle\rho\rangle$ or $\rho_{\mathrm{vac}} = \langle\rho\rangle + \Lambda/8\pi G$. Note at this point that only the effective cosmological constant, Λ_{eff}, is observable, not Λ, so the latter quantity may be referred to as a "bare". The two approaches are, of course, equivalent for a given theory (Vishwakarma [125]). For detailed discussions, the readers are advised to see the references: Carroll et al. [161]; Abdussattar and Vishwakarma [162]; Peebles [163]; Sahni and Starobinsky [20]; Padmanabhan [164, 165].

Figure 27 is the plot of the cosmological constant Λ versus time t. We observe that cosmological parameter is a decreasing function of time and it approaches a small positive value at late time (i.e., at present epoch). Recent cosmological observations [1–5] suggest the existence of a positive cosmological constant Λ with the magnitude $\Lambda(G\hbar/c^3) \approx 10^{-123}$. These observations on the magnitude and redshift of type Ia supernova suggest that our universe may be an accelerating one with induced cosmological density through the cosmological Λ-term. Thus, the nature of Λ in our derived DE model is supported by recent observations.

Figure 28 is a plot of deceleration parameter q versus time t. From this figure, it is observed that q decreases very rapidly and reaches values -1, and then it remains constant -1 (like de Setter universe). From this figure, we observe also that the DE model, for $0 < n < 1.5$, evolves from the matter dominated era to quintessence era and ultimately approaches cosmological constant era where, as for $n \geqslant 1.5$, the universe evolves from quintessence to cosmological constant era. It is worth mentioning here that for $n < 1.5$, transition of the universe takes place from the early decelerating phase to the recent accelerating phase where, as for $n \geqslant 1.5$, the expansion of the universe is always accelerating.

From this analysis, we conclude that it is the choice of scale factor which makes the model inflationary at the early stages of the universe and radia-
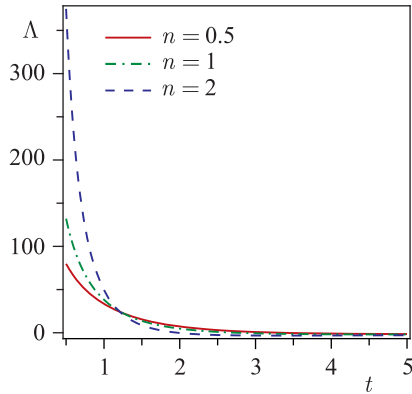
Fig. 27. The cosmological constant Λ versus t. Here $\ell_0 = 0.1$, $m = 1$
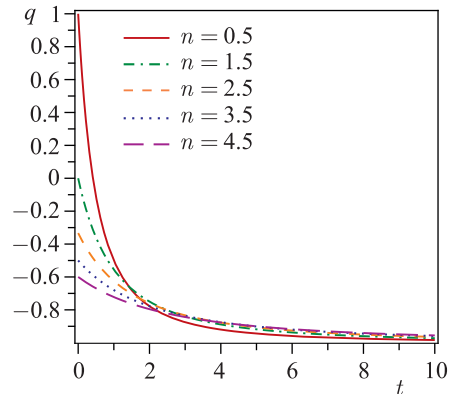
Fig. 28. The deceleration parameter q versus t

tion/matter dominance phase before the DE era. From Eq. (200), we observe that when $t \to 0$, the expansion scalar θ becomes infinity which indicates the inflationary scenario. Also from Fig. 28, we observe that before $t \approx 1$, $q > 0$, and this indicates radiation/matter dominance era of the universe. However, after $t \approx 1$, $q < 0$ which indicates the DE dominated era. The solution in our model does not blow up at any given epoch for the choice of the *ansatz* (195). Hence our derived model is physically acceptable.

The Cosmic Microwave Background (CMB) is also considered to be a major experimental evidence which supports the present models of the observed universe, and from this CMB observations several scientists found the signature of anisotropy. Based on these studies and observations, one may not preclude the possibility that our universe is anisotropic. We have already discussed this scenario in Introduction. The background solution is stable against the perturbation of the graviton field [166].

To find another new solution, we take the following *ansatz* for the scale factor, where the increase in terms of time evolution is

$$a(t) = -\frac{1}{t} + t^2. \tag{212}$$

The above choice of scale factor yields a time-dependent deceleration parameter and the corresponding solutions are stable

$$q = -2\left(\frac{t^3 - 1}{2t^3 + 1}\right)^2. \tag{213}$$

In this case, we obtain the expressions for metric functions as follows:

$$B(t) = \ell_4 \left(-\frac{1}{t} + t^2\right)^{\frac{3}{(m+2)}}, \tag{214}$$

$$C(t) = \ell_5 \left(-\frac{1}{t} + t^2\right)^{\frac{3}{(m+2)}}, \tag{215}$$

$$A(t) = \ell_6 \left(-\frac{1}{t} + t^2\right)^{\frac{3m}{(m+2)}}, \tag{216}$$

where, $\ell_4 = 1^{-\frac{1}{(m+2)}}$, $\ell_5 = \ell\ell_4$, $\ell_6 = \ell_4^m$, and 1 is an integrating constant.

Hence, the model (165) reduces to

$$ds^2 = -dt^2 + \ell_6^2 \left(-\frac{1}{t} + t^2\right)^{\frac{6m}{(m+2)}} dx^2 + \ell_4^2 \left(-\frac{1}{t} + t^2\right)^{\frac{6}{(m+2)}} dy^2 +$$
$$+ \ell_5^2 \left(-\frac{1}{t} + t^2\right)^{\frac{6}{(m+2)}} dz^2. \tag{217}$$

The expressions for the Hubble parameter (H), scalar of expansion (θ), shear scalar (σ), spatial volume (V), and the average anisotropy parameter (A_m) for the model (217) are given by

$$\theta = 3H = \frac{3}{t} \left(\frac{2t^3 + 1}{t^3 - 1}\right), \tag{218}$$

$$\sigma^2 = 3\left[\left(\frac{m-1}{m+2}\right)\frac{(2t^3 + 1)}{(t^3 - 1)t}\right]^2, \tag{219}$$

$$V = \left(-\frac{1}{t} + t^2\right)^3, \tag{220}$$

$$A_m = 2\left(\frac{m-1}{m+2}\right)^2. \tag{221}$$

From Eq. (218), we observe that when $t \to 0$, $\theta \to \infty$ and this indicates the inflationary scenario at early stages of the universe. Since $\sigma^2/\theta^2 \neq 0$ for all values of m except for $m = 1$, hence the model is anisotropic except for $m = 1$. The dynamics of the mean anisotropy parameter depends on the value of m. The mean anisotropic parameter is constant. We observed that when $m = -2$, $A_m \to \infty$ and for $m = 1$, $A_m = 0$. Thus, the observed isotropy of the universe can be achieved in the phantom model (see Fig. 32).

The energy density of the fluid, the EoS parameter ω, and skewness parameters δ (or γ) (i.e., deviations from ω along y-axis and z-axis) are obtained as

$$\rho = \frac{9(2m+1)}{(m+2)^2} \frac{(2t^3+1)^2}{(t^3-1)^2 t^2} - \ell_0 \left(-\frac{1}{t} + t^2 \right)^{-\frac{6m}{(m+2)}},$$ (222)

$$\omega = \frac{\dfrac{27}{(m+2)^2} \dfrac{(2t^3+1)^2}{(t^3-1)^2 t^2} - \dfrac{6}{(m+2)} \dfrac{(2t^6+8t^3-1)}{(t^3-1)^2 t^2} + \ell_0 \left(-\dfrac{1}{t} + t^2 \right)^{-\frac{6m}{(m+2)}}}{\ell_0 \left(-\dfrac{1}{t} + t^2 \right)^{-\frac{6m}{(m+2)}} + \dfrac{9(2m+1)}{(m+2)^2} \dfrac{(2t^3+1)^2}{(t^3-1)^2 t^2}},$$ (223)

$$\delta = \gamma = \frac{6 \left(\dfrac{m-1}{m+2} \right) \dfrac{(5t^6+2t^3+2)}{(t^3-)^2 t^2} - 2\ell_0 \left(-\dfrac{1}{t} + t^2 \right)^{-\frac{6m}{(m+2)}}}{\ell_0 \left(-\dfrac{1}{t} + t^2 \right)^{-\frac{6m}{(m+2)}} - \dfrac{9(2m+1)}{(m+2)^2} \dfrac{(2t^3+1)^2}{(t^3-1)^2 t^2}},$$ (224)

where $\mathfrak{l}_0 = 1/\ell_6^2$.

So, if the present work is compared with experimental results [10, 21, 50, 51], then one can conclude that the limit of ω provided by Eq. (223) may be accommodated with the acceptable range of EoS parameter. Also it is observed that at $t = t_c$, ω vanishes, where t_c is a critical time given by the following relation:

$$\frac{27}{(m+2)^2} \frac{(2t_c^3+1)^2}{(t_c^3-1)^2 t_c^2} - \frac{6}{(m+2)} \frac{(2t_c^6+8t_c^3-1)}{(t_c^3-1)^2 t_c^2} + \ell_0 \left(-\frac{1}{t_c} + t_c^2 \right)^{-\frac{6m}{(m+2)}} = 0.$$ (225)

Thus, for this particular time, our model represents a dusty universe. We also note that the earlier real matter at $t \leqslant t_c$, where $\omega \geqslant 0$, later on at $t > t_c$, where $\omega < 0$, is converted to the dark-energy dominated phase of universe.

From Eq. (222), we note that energy density of the fluid $\rho(t)$ is a decreasing function of time and $\rho \geqslant 0$ when

$$\frac{(2t^3+1)^2}{(t^3-1)^2 t^2} \left(-\frac{1}{t} + t^2 \right)^{\frac{6m}{(m+2)}} \geqslant \frac{\ell_0(m+2)^2}{9(2m+1)}.$$ (226)

Figure 29 is the plot of energy density of the fluid (ρ) versus time t. Here we observe that ρ is a positive decreasing function of time and it approaches zero as $t \to \infty$.

Figure 30 depicts the variation of EoS parameter (ω) versus cosmic time (t) in evolution of the universe, as a representative case with appropriate choice of constants of integration and other physical parameters using reasonably well-known situations. From Fig. 30, we observe as follows:

(i) For $m \leqslant 0.5$, the evolution of the universe starts from quintessence era ($\omega > -1$) and approaches to phantom region ($\omega < -1$).

(ii) For $1 \leqslant m < 2$, the universe evolves from phantom region ($\omega < -1$), then crosses PDL and ultimately approaches quintessence region ($\omega > -1$).

(iii) For $2 \leqslant m \leqslant 3$, the evolution of the universe commence from phantom region ($\omega < -1$), then crosses PDL and then skip over to nondark region.

(iv) For $3 \leqslant m$, the evolution of the universe begins from quintessence era ($\omega > -1$) and ultimately passes over to nondark region.

(v) For $m = 1$, we get $\omega \approx -0.65$ which is consistent with SNe Ia data $-1.67 < \omega < -0.62$ (Knop et al. [50]).

(vi) For $m = 0.5$, we get $\omega \approx -1.1$ which is reproducible with current observational realm [10, 21, 50, 51].
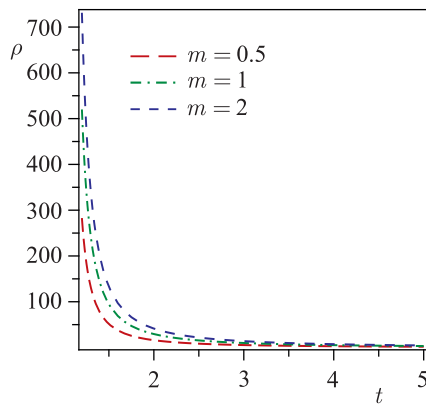
Fig. 29. The energy density ρ versus t. Here $\ell_0 = 0.1$
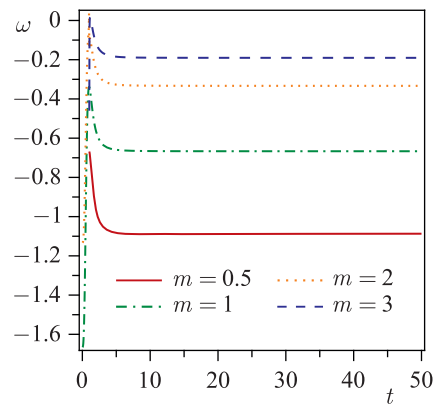
Fig. 30. The EoS parameter ω versus t. Here $\ell_0 = 0.1$

The cosmological constant is obtained as

$$\Lambda = \frac{3(4m^2 + 10m + 13)}{(m+2)^2} \frac{(2t^3 + 1)^2}{(t^3 - 1)^2 t^2} + \ell_0 \left(-\frac{1}{t} + t^2 \right)^{\frac{-6m}{(m+2)}}. \tag{227}$$

From Eq. (227), we observe that Λ is a decreasing function of time and it is always positive when

$$\frac{(2t^3 + 1)^2}{(t^3 - 1)^2 t^2} \left(-\frac{1}{t} + t^2 \right)^{\frac{6m}{(m+2)}} > -\frac{\ell_0 (m+2)^2}{3(4m^2 + 10m + 13)}. \tag{228}$$

Figure 31 is the plot of cosmological constant Λ versus time t. It is observed that in all cases cosmological parameter is a decreasing function of time and it
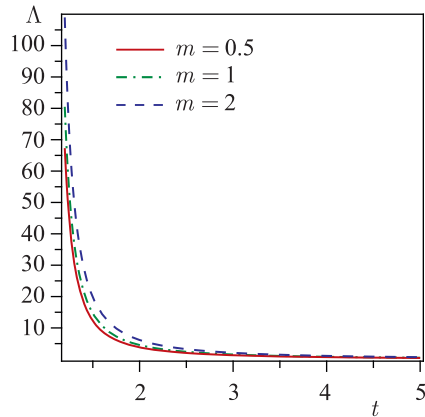
Fig. 31. The cosmological constant Λ versus t. Here $\ell_0 = 0.1$
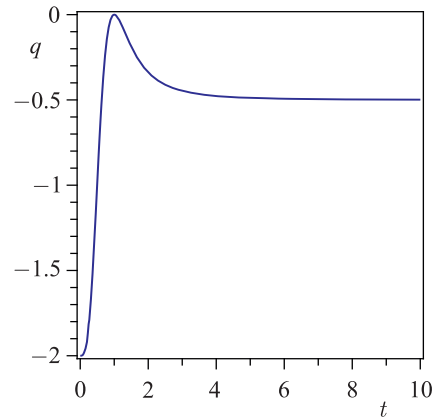
Fig. 32. The deceleration parameter q versus t

approaches a small positive value at late time (i.e., at present epoch). Thus, the nature of Λ in this derived DE model is also in good agreement with the recent observations [1–5].

Figure 32 is the plot of deceleration parameter q versus time t. From the figure we observe that the expansion of the universe starts from accelerating phase, and the rate of expansion decreases with time and it stops and again starts accelerating to approach -0.5 which is very close to the value (≈ -0.7) predicted by the observations (Riess et al. [5]; Virey et al. [167]).

A convenient method to describe models close to ΛCDM is based on the cosmic jerk parameter j, a dimensionless third derivative of the scale factor with respect to the cosmic time [152–156]. A deceleration-to-acceleration transition occurs for models with a positive value of j_0 and negative q_0. Flat ΛCDM models have a constant jerk $j = 1$. The jerk parameter in this case is obtained. In this case, we obtain the jerk parameter as

$$j(t) = \frac{2t^5 + 2t^4 - 2t^2 - t - 2}{(t+1)(1+t^2)}. \tag{229}$$

This value is consistent with observational value $j \simeq 2.16$ obtained from the combination of three kinematical data sets: the gold sample of type Ia supernovae [5], the SNIa data from the SNLS project [136], and the X-ray galaxy cluster distance measurements [157] for $t = 1.50$.

A new class of anisotropic B-VI$_0$ DE models with variable EoS parameter ω has been investigated using time-dependent deceleration parameter. In literature, it is plebeian to practice a constant deceleration parameter. Now for a universe which was decelerating in past and accelerating at present epoch, the DP must

show signature flipping as is already discussed in previous sections. Therefore our consideration of DP to be variable is physically justified.

The main features of the models are as follows:

• DE models present the dynamics of EoS parameter ω whose range is in good agreement with the acceptable range by the recent observations [10, 21, 50, 51].

• We obtain cosmological constant dominated universe, quintessence and phantom fluid dominated universe (Chevallier and Polarski [59]), representing the different phases of the universe through-out the evolving process for different cosmic times. These fits suggest that $\omega > -1$ for a long (quintessence-like) period in the past, and at the same time they suggest that the universe has just entered a phantom phase $\omega < -1$ near our present.

• Unlike Robertson–Walker (RW) metric, Bianchi type metrics can admit a DE that wields an anisotropic EoS parameter according to the characteristics. Therefore, one cannot rule out the possibility of anisotropic nature of DE in the framework of B-VI$_0$ space-time.

• In the first case, the observed isotropy of the universe can be achieved in cosmological constant model (see Fig. 26), whereas in the second case, the observed isotropy of the universe can be achieved in phantom model (see Fig. 30). Thus, Bianchi type-VI$_0$ models, which remain anisotropic, are of preferably academical interest.

• Our DE models are of great importance in the sense that the nature of decaying vacuum energy density $\Lambda(t)$ is supported by recent cosmological observations [1–5].

• Though there are many suspects (candidates) such as cosmological constant, vacuum energy, scalar field, brane world, cosmological nuclear-energy, etc., as reported in the vast literature for DE, the proposed models in this paper favour EoS parameter as a possible suspect for the DE.

• The cosmic jerk parameter in our derived models is also found to be in good agreement with the recent data of astrophysical observations.

• For different choice of n, we can generate a class of DE models in Bianchi type-VI$_0$ space-time. It is observed that such DE models are also in good harmony with current observations. Our study is continued and we shall generate some other interesting physically viable models for other values of n.

• Our corresponding solutions have inflationary scenario at the early stages of the universe and also radiation/matter era before DE era.

• Our corresponding solutions are physically acceptable and stable.

Thus, the solutions demonstrated in this section may be useful for better understanding of the characteristic of anisotropic DE in the evolution of the universe within the framework of Bianchi type-VI$_0$ space-time.

CONCLUSIONS

In this review article, we have studied anisotropic Bianchi type-I, II, III, V and VI$_0$ space-times in connection with dark-energy models. The main study in this article has been concentrated to observe whether our derived results are consistent with recent results of astrophysical observations or not. We find that the results obtained in different Bianchi type space-times are in good agreement with recent observations. Hence, one cannot rule out the possibility of anisotropic nature of dark energy in the framework of Bianchi type space-times.

REFERENCES

1. *Riess A. G. et al.* Observational Evidence from Supernovae for an Accelerating Universe and a Cosmological Constant // Astron. J. 1998. V. 116. P. 1009–1038.

2. *Perlmutter S. et al.* Discovery of a Supernova Explosion at Half the Age of the Universe // Nature. 1998. V. 391. P. 51–54.

3. *Perlmutter S. et al.* Measurements of Ω and Λ from 42 High-Redshift Supernovae // Astrophys. J. 1999. V. 517. P. 565–586.

4. *Tonry J. L. et al.* Cosmological Results from High-z Supernovae // Astrophys. J. 2003. V. 594. P. 1–24.

5. *Riess A. G. et al.* Type Ia Supernova Discoveries at $z > 1$ from the Hubble Space Telescope: Evidence for Past Deceleration and Constraints on Dark Energy Evolution // Astrophys. J. 2004. V. 607. P. 665–687.

6. *Clocchiatti A. et al.* Hubble Space Telescope and Ground-Based Observations of Type Ia Supernovae at Redshift 0.5: Cosmological Implications // Astrophys. J. 2006. V. 642. P. 1–21.

7. *Bennett C. L. et al.* First Year Wilkinson Microwave Anisotropy Probe (WMAP) Observations: Preliminary Maps and Basic Results // Astrophys. J. Suppl. Ser. 2003. V. 148. P. 1.

8. *de Bernardis P. et al.* A Flat Universe from High-Resolution Maps of the Cosmic Microwave Background Radiation // Nature. 2000. V. 404. P. 955–959.

9. *Hanany S. et al.* MAXIMA-1: A Measurement of the Cosmic Microwave Background Anisotropy on Angular Scales of 10'-5A // Astrophys. J. 2000. V. 545. L5–L9.

10. *Tegmark M. et al.* Cosmological Parameters from SDSS and WMAP // Phys. Rev. D. 2004. V. 69. P. 103501.

11. *Tegmark M. et al.* The 3D Power Spectrum of Galaxies from the SDSS // Astrophys. J. 2004. V. 606. P. 702–740.

12. *Spergel D. N. et al.* First-Year Wilkinson Microwave Anisotropy Probe (WMAP) Observations: Determination of Cosmological Parameters // Astrophys. J. Suppl. 2003. V. 148. P. 175–194.

13. *Seljak U. et al.* Cosmological Parameter Analysis Including SDSS Lyα Forest and Galaxy Bias: Constraints on the Primordial Spectrum of Fluctuations, Neutrino Mass, and Dark Energy // Phys. Rev. D. 2005. V. 71. P. 103515.

14. *Adelman-McCarthy J. K. et al. (SDSS Collab.).* The Fourth Data Release of the Sloan Digital Sky Survey // Astrophys. J. Suppl. 2006. V. 162. P. 38–48.

15. *Knop R. A. et al.* New Constraints on Ω_M, Ω_Λ, and w from an Independent Set of Eleven High-Redshift Supernovae Observed with HST // Astrophys. J. 2003. V. 598. P. 102.

16. *Allen S. W. et al.* Constraints on Dark Energy from Chandra Observations of the Largest Relaxed Galaxy Clusters // Mon. Not. Roy. Astron. Soc. 2004. V. 353. P. 457–467.

17. *Caldwell R. R. et al.* Sudden Gravitational Transition // Phys. Rev. D. 2006. V. 73. P. 023513.

18. *Rincon P.* New Method Confirms Dark Energy. http://www.bbc.co.uk/news/science-environment-1346296. BBC News. 19 May, 2011.

19. *Overduin J. M., Cooperstock F. I.* Evolution of the Scale Factor with a Variable Cosmological Term // Phys. Rev. D. 1998. V. 58. P. 043506.

20. *Sahni V., Starobinsky A. A.* The Case for a Positive Cosmological Lambda-Term // Intern. J. Mod. Phys. D. 2000. V. 9. P. 373–444.

21. *Komatsu E. et al. (WMAP Collab.).* Five-Year Wilkinson Microwave Anisotropy Probe (WMAP) Observations: Cosmological Interpretation // Astrophys. J. Suppl. Ser. 2009. V. 180. P. 330–376.

22. *Kachru S. et al.* de Sitter Vacua in String Theory // Phys. Rev. D. 2003. V. 68. P. 046005.

23. *Weinberg S.* The Cosmological Constant Problem // Rev. Mod. Phys. 1989. V. 61. P. 1–23.

24. *Wetterich C.* Cosmology and the Fate of Dilatation Symmetry // Nucl. Phys. B. 1988. V. 302. P. 668–696.

25. *Ratra B., Peebles P. J. E.* Cosmological Consequences of a Rolling Homogeneous Scalar Field // Phys. Rev. D. 1988. V. 37. P. 3406–3427.

26. *Khoury J., Weltman A.* Chameleon Fields: Awaiting Surprises for Tests of Gravity in Space // Phys. Rev. Lett. 2004. V. 93. P. 171104.

27. *Chiba T., Okabe T., Yamaguchi M.* Kinetically Driven Quintessence // Phys. Rev. D. 2000. V. 62. P. 023511.

28. *Armendariz-Picon C., Mukhanov V., Steinhardt P. J.* Dynamical Solution to the Problem of a Small Cosmological Constant and Late-Time Cosmic Acceleration // Phys. Rev. Lett. 2000. V. 85. P. 4438–4441.

29. *Armendariz-Picon C., Damour T., Mukhanov V.* k-Inflation // Phys. Lett. B. 1999. V. 458. P. 209–218.

30. *Capozziello S.* Curvature Quintessence // Intern. J. Mod. Phys. D. 2002. V. 11. P. 483–492.

31. *Carroll S. M. et al.* Is Cosmic Speed-Up Due to New Gravitational Physics? // Phys. Rev. D. 2004. V. 70. P. 043528.

32. *Dolgov A. D., Kawasaki M.* Can Modified Gravity Explain Accelerated Cosmic Expansion? // Phys. Lett. B. 2003. V. 573. P. 1–4.

33. *Nojiri S., Odintsov S. D.* Modified Gravity with Negative and Positive Powers of Curvature: Unification of Inflation and Cosmic Acceleration // Phys. Rev. D. 2003. V. 68. P. 123512.

34. *Nojiri S., Odintsov S. D.* The Minimal Curvature of the Universe in Modified Gravity and Conformal Anomaly Resolution of the Instabilities // Mod. Phys. Lett. A. 2004. V. 19. P. 627–638.

35. *Abdalla M. C. B., Nojiri S., Odintsov S. D.* Consistent Modified Gravity: Dark Energy, Acceleration and the Absence of Cosmic Doomsday // Class. Quant. Grav. 2005. V. 22. P. L35.

36. *Mena O., Santiago J., Weller J.* Constraining Inverse-Curvature Gravity with Supernovae // Phys. Rev. Lett. 2006. V. 96. P. 041103.

37. *Padmanabhan T.* Accelerated Expansion of the Universe Driven by Tachyonic Matter // Phys. Rev. D. 2002. V. 66. P. 021301.

38. *Sen A.* Tachyon Matter // JHEP. 2002. V. 0207. P. 065.

39. *Peebles P. J. E., Vilenkin A.* Quintessential Inflation // Phys. Rev. D. 1999. V. 59. P. 063505.

40. *Srivastava S. K.* Future Universe with $w < -1$ without Big Smash // Phys. Lett. B. 2005. V. 619. P. 1–4.

41. *Jackiw R.* A Particle Field Theorist's Lectures on Super Symmetric, Non-Abelian Field Mechanics and D-Branes. arXiv:physics/0010042. 2000.

42. *Bertolami O. et al.* Latest Supernova Data in the Framework of Generalized Chaplygin Gas Model // Mon. Not. Roy. Astron. Soc. 2004. V. 353. P. 329.

43. *Bento M. C., Bertolami O., Sen A. A.* Generalized Chaplygin Gas, Accelerated Expansion and Dark Energy–Matter Unification // Phys. Rev. D. 2002. V. 66. P. 043507.

44. *Bilic N., Tupper G. B., Viollier R. D.* Unification of Dark Matter and Dark Energy: the Inhomogeneous Chaplygin Gas // Phys. Lett. B. 2002. V. 353. P. 17–21.

45. *Avelino C. et al.* Alternatives to Quintessence Model Building // Phys. Rev D. 2003. V. 67. P. 023511.

46. *Gupta R. C., Pradhan A.* Genesis of Dark Energy: Dark Energy as a Consequence of Release and Two-Stage Tracking of Cosmological Nuclear Energy // Intern. J. Theor. Phys. 2010. V. 49. P. 821–834.

47. *Carroll S. M., Hoffman M.* Can the Dark Energy Equation-of-State Parameter w Be Less than -1? // Phys. Rev. D. 2003. V. 68. P. 023509.

48. *Steinhardt P. J., Wang L. M., Zlatev I.* Cosmological Tracking Solutions // Phys. Rev. D. 1999. V. 59. P. 123504.

49. *Caldwell R. R.* A Phantom Menace? Cosmological Consequences of a Dark Energy Component with Super-Negative Equation of State // Phys. Lett. B. 2002. V. 545. P. 23–29.

50. *Knop R. A. et al.* Spatially Resolved Near-Infrared Spectroscopy of Seyfert 2 Galaxies Mk 1066, NGC 2110, NGC 4388, and Mk 3 // Astron. J. 2001. V. 122. P. 764–791.

51. *Hinshaw G. et al.* Five-Year Wilkinson Microwave Anisotropy Probe (WMAP) Observations: Data Processing, Sky Maps, and Basic Results // Astrophys. J. Suppl. Ser. 2009. V. 180. P. 225–245.

52. *Kujat J. et al.* Prospects for Determining the Equation of State of the Dark Energy: What Can Be Learned from Multiple Observables? // Astrophys. J. 2002. V. 572. P. 1–14.

53. *Bartelmann M. et al.* Evolution of Dark-Matter Haloes in a Variety of Dark-Energy Cosmologies // New Astron. Rev. 2005. V. 49. P. 199–203.

54. *Yadav A. K.* Some Anisotropic Dark Energy Models in Bianchi Type-V Space-Time // Astrophys. Space Sci. 2011. V. 335. P. 565–575.

55. *Jimenez R.* The Value of the Equation of State of Dark Energy // New Astron. Rev. 2003. V. 47. P. 761–767.

56. *Das A. et al.* Cosmology with Decaying Tachyon Matter // Phys. Rev. D. 2005. V. 72. P. 043528.

57. *Huterer D., Turner M. S.* Probing Dark Energy: Methods and Strategies // Phys. Rev. D. 2001. V. 64. P. 123527.

58. *Weller J., Albrecht A.* Future Supernovae Observations as a Probe of Dark Energy // Phys. Rev. D. 2002. V. 65. P. 103512.

59. *Chevallier M., Polarski D.* Accelerating Universes with Dark Matter // Intern. J. Mod. Phys. D. 2001. V. 10. P. 213.

60. *Linder E. V.* Exploring the Expansion History of the Universe // Phys. Rev. Lett. 2003. V. 90. P. 91301.

61. *Linder E. V.* The Dynamics of Quintessence, the Quintessence of Dynamics // Gen. Rel. Grav. 2008. V. 40. P. 329–356.

62. *Rahaman F., Bhui B., Bhui B. C.* Cosmological Model with a Viscous Fluid in a Kaluza–Klein Metric // Astrophys. Space Sci. 2006. V. 301. P. 47–49.

63. *Mukhopadhyay U., Ghosh P. P., Choudhury S. B. D.* Λ-CDM Universe: A Phenomenological Approach with Many Possibilities // Intern. J. Mod. Phys. D. 2008. V. 17. P. 301–309.

64. *Setare M. R.* The Holographic Dark Energy in Nonflat Brans–Dicke Cosmology // Phys. Lett. B. 2007. V. 644. P. 99–103.

65. *Setare M. R.* Interacting Holographic Phantom // Eur. Phys. J. C. 2007. V. 50. P. 991–998.

66. *Setare M. R.* Interacting Holographic Generalized Chaplygin Gas Model // Phys. Lett. B. 2007. V. 654. P. 1–6.

67. *Setare M. R., Vagenas E. C.* The Cosmological Dynamics of Interacting Holographic Dark Energy Model // Intern. J. Mod. Phys. D. 2009. V. 18. P. 147–1557.

68. *Cai Y.-F., Saridakis E. N., Setare M. R.* Quintom Cosmology: Theoretical Implications and Observations // Phys. Rep. 2010. V. 493. P. 1–60.

69. *Jamil M., Saridakis E. N., Setare M. R.* Thermodynamics of Dark Energy Interacting with Dark Matter and Radiation // Phys. Rev. D. 2010. V. 81. P. 023007.

70. *Ray S. et al.* Variable Equation of State for Generalized Dark Energy Model // Intern. J. Theor. Phys. 2011. V. 50. P. 2687–2696.

71. *Akarsu Ö., Kilinc C. B.* LRS Bianchi Type-I Models with Anisotropic Dark Energy and Constant Deceleration Parameter // Gen. Rel. Grav. 2010. V. 42. P. 119–140.

72. *Akarsu Ö., Kilinc C. B.* Bianchi Type-III Models with Anisotropic Dark Energy // Ibid. P. 763–775.

73. *Akarsu Ö., Kilinc C. B.* De Sitter Expansion with Anisotropic Fluid in Bianchi Type-I Space-Time // Astrophys. Space Sci. 2010. V. 326. P. 315–322.

74. *Akarsu Ö., Kilinc C. B.* Some Anisotropic Universes in the Presence of Imperfect Fluid Coupling with Spatial Curvature // Intern. J. Theor. Phys. 2011. V. 50. P. 1962–1977.

75. *Yadav A. K., Rahaman F., Ray S.* Dark Energy Models with Variable Equation of State Parameter // Intern. J. Theor. Phys. 2011. V. 50. P. 871–781.

76. *Yadav A. K., Yadav L.* Bianchi Type-III Anisotropic Dark Energy Models with Constant Deceleration Parameter // Ibid. P. 218–227.

77. *Yadav A. K., Saha B.* LRS Bianchi-I Anisotropic Cosmological Model with Dominance of Dark Energy // Astrophys. Space Sci. 2012. V. 337. P. 759–765.

78. *Pradhan A., Amirhashchi H.* Dark Energy Model in Anisotropic Bianchi Type-III Space-Time with Variable EoS Parameter // Astrophys. Space Sci. 2011. V. 332. P. 441–448.

79. *Pradhan A., Amirhashchi H.* Accelerating Dark Energy Models in Bianchi Type-V Space-Time // Mod. Phys. Lett. A. 2011. V. 26. P. 2261–2275.

80. *Pradhan A., Amirhashchi H., Saha B.* Bianchi Type-I Anisotropic Dark Energy Model with Constant Deceleration Parameter // Intern. J. Theor. Phys. 2011. V. 50. P. 2923–2938.

81. *Pradhan A., Amirhashchi H., Jaiswal R.* A New Class of LRS Bianchi Type-II Dark Energy Models with Variable EoS Parameter // Astrophys. Space Sci. 2011. V. 334. P. 249–260.

82. *Pradhan A. et al.* Dark Energy Models with Anisotropic Fluid in Bianchi Type-VI$_0$ Space-Time with Time-Dependent Deceleration Parameter // Astrophys. Space Sci. 2012. V. 337. P. 401–413.

83. *Amirhashchi H., Pradhan A., Saha B.* An Interacting Two-Fluid Scenario for Dark Energy in FRW Universe // Chin. Phys. Lett. 2011. V. 28. P. 039801.

84. *Amirhashchi H., Pradhan A., Zainuddin H.* Interacting Two-Fluid Viscous Dark Energy Models in Nonflat Universe // Res. Astron. Astrophys. 2013. V. 13. P. 129–138.

85. *Amirhashchi H., Pradhan A., Zainuddin H.* An Interacting and Noninteracting Two-Fluid Dark Energy Models in FRW Universe with Time-Dependent Deceleration Parameter // Intern. J. Theor. Phys. 2011. V. 50. P. 3529–3543.

86. *Amirhashchi H., Pradhan A., Saha B.* Variable Equation of State for Bianchi Type-VI$_0$ Dark Energy Models // Astrophys. Space Sci. 2011. V. 333. P. 295–303.

87. *Kumar S.* Anisotropic Model of Dark Energy Dominated Universe with Hybrid Expansion Law // Gravitation and Cosmology. 2013. V. 19. P. 284–287.

88. *Kumar S.* Some FRW Models of Accelerating Universe with Dark Energy // Astrophys. Space Sci. 2011. V. 332. P. 449–454.

89. *Kumar S., Akarsu Ö.* Bianchi Type-II Models in the Presence of Perfect Fluid and Anisotropic Dark Energy // Eur. Phys. J. Plus. 2012. V. 127. P. 64.

90. *Kumar S., Yadav A. K.* Some Bianchi Type-V Models of Accelerating Universe with Dark Energy // Mod. Phys. Lett. A. 2011. V. 26. P. 647–659.

91. *Kumar S., Singh C. P.* Anisotropic Dark Energy Models with Constant Deceleration Parameter // Gen. Rel. Grav. 2011. V. 43. P. 1427–1442.

92. *Nojiri S., Odintsov S. D.* Introduction to Modified Gravity and Gravitational Alternative for Dark Energy // Intern. J. Geom. Meth. Mod. Phys. 2007. V. 4. P. 115–146.

93. *Nojiri S., Odintsov S. D.* Unified Cosmic History in Modified Gravity: From $F(R)$ Theory to Lorentz Noninvariant Models // Phys. Rep. 2011. V. 505. P. 59–144.

94. *Nojiri S., Odintsov S. D.* Inhomogeneous Equation of State of the Universe: Phantom Era, Future Singularity, and Crossing the Phantom Barrier // Phys. Rev. D. 2005. V. 72. P. 023003.

95. *Nojiri S., Odintsov S. D.* The Oscillating Dark Energy: Future Singularity and Coincidence Problem // Phys. Lett. B. 2006. V. 637. P. 139–148.

96. *Birch P.* Is the Universe Rotating? // Nature. 1982. V. 298. P. 451–454.

97. *Jain P., Ralston J. P.* Anisotropy in the Distribution of Galactic Radio Polarizations // Mod. Phys. Lett. A. 1999. V. 14. P. 417–432.

98. *Jain P., Narain G., Sarala S.* Large Scale Alignment of Optical Polarizations from Distant QSOs Using Coordinate Invariant Statistics // Mon. Not. Roy. Astron. Soc. 2004. V. 347. P. 394.

99. *Hutsemékers D.* Evidence for Very Large-Scale Coherent Orientations of Quasar Polarization Vectors // Astron. Astrophys. 1998. V. 332. P. 410–428.

100. *Hutsemékers D., Lamy H.* Confirmation of the Existence of Coherent Orientations of Quasar Polarization Vectors on Cosmological Scales // Astron. Astrophys. 2001. V. 367. P. 381.

101. *Ralston J. P., Jain P.* The Virgo Alignment Puzzle in Propagation of Radiation on Cosmological Scales // Intern. J. Mod. Phys. D. 2004. V. 13. P. 1857–1878.

102. *Tegmark M., de Oliveira-Costa A., Hamilton A. J.* High Resolution Foreground Cleaned CMB Map from WMAP // Phys. Rev. D. 2003. V. 68. P. 123523.

103. *de Oliveira-Costa A. et al.* Significance of the Largest Scale CMB Fluctuations in WMAP // Phys. Rev. D. 2004. V. 69. P. 063516.

104. *Jain P., Modgil M. S., Ralston J. P.* Search for Global Metric Anisotropy in Type Ia Supernova Data // Mod. Phys. Lett. A. 2007. V. 22. P. 1153–1165.

105. *Cooke R., Lynden-Bell D.* Does the Universe Accelerate Equally in All Directions? // Mon. Not. Roy. Astron. Soc. 2010. V. 401. P. 1409–1414.

106. *Cooray A., Holz D. E., Caldwell R.* Measuring Dark Energy Spatial Inhomogeneity with Supernova Data // JCAP. 2010. V. 11. P. 015.

107. *Atrio-Barandela F. et. al.* Probing the Dark Flow Signal in Nine-Year WMAP and Planck Cosmic Microwave Background Maps. arXiv:1411.4180v1 [astro-ph.CO].

108. *Larson D. et. al.* Comparing Planck and WMAP: Maps, Spectra, and Parameters. arXiv:1409.7718v1 [astro-ph.CO].

109. *Ellis G. F. R.* The Bianchi Models: Then and Now // Gen. Rel. Grav. 2006. V. 38. P. 1003–1015.

110. *Ellis G. F. R.* Cosmological Models // Modern Cosmology. Bristol: Inst. of Phys. Publ., 2002. P. 108–158.

111. *Komatsu E. et al.* Seven-Year Wilkinson Microwave Anisotropy Probe (WMAP) Observations: Cosmological Interpretation // Astrophys. J. Suppl. 2011. V. 192. P. 18.

112. *Spergel D. N. et al.* Wilkinson Microwave Anisotropy Probe (WMAP) Three-Year Results: Implications for Cosmology // Astrophys. J. Suppl. 2007. V. 170. P. 377.

113. *Peiris H. V. et al.* First-Year Wilkinson Microwave Anisotropy Probe (WMAP) Observations: Implications for Inflation // Astrophys. J. Suppl. Ser. 2003. V. 148. P. 213.

114. *de Oliveira-Costa A. et al.* Significance of the Largest Scale CMB Fluctuations in WMAP // Phys. Rev. D. 2004. V. 69. P. 063516.

115. *Schwarz D. J. et al.* Is the Low-l Microwave Background Cosmic? // Phys. Rev. Lett. 2004. V. 93. 221301.

116. *Cruz M. et al.* The Non-Gaussian Cold Spot in the Three-Year WMAP Data // Astrophys. J. 2007. V. 655. P. 11–20.

117. *Hoftuft J. et al.* Increasing Evidence for Hemispherical Power Asymmetry in the Five-Year WMAP Data // Astrophys. J. 2009. V. 699. V. 985–989.

118. *Bennett C. L. et al.* Seven-Year Wilkinson Microwave Anisotropy Probe (WMAP) Observations: Are There Cosmic Microwave Background Anomalies? // Astrophys. J. Suppl. Ser. 2011. V. 192. P. 17.

119. *Berman M. S.* A Special Law of Variation for Hubble Parameter // Nuovo Cim. B. 1983. V. 74. P. 182–186.

120. *Berman M. S., Gomide F. M.* Cosmological Models with Constant Deceleration Parameter // Gen. Rel. Grav. 1988. V. 20. P. 191–198.

121. *Singh C. P., Kumar S.* Bianchi Type-II Inflationary Models with Constant Deceleration Parameter in General Relativity // Pramana J. Phys. 2007. V. 68. P. 707–720.

122. *Singh C. P., Kumar S.* Bianchi Type-II Space-Times with Constant Deceleration Parameter in Self-Creation Cosmology // Astrophys. Space Sci. 2007. V. 310. P. 31–39.

123. *Singh C. P., Kumar S.* Bianchi Type-II Cosmological Models with Constant Deceleration Parameter // Intern. J. Mod. Phys. D. 2006. V. 15. P. 419–438.

124. *Pradhan A., Jotania K.* Some Exact Bianchi Type-V Perfect Fluid Cosmological Models with Heat Flow and Decaying Vacuum Energy Density: Expressions for Some Observable Quantities // Intern. J. Theor. Phys. 2010. V. 49. P. 1719–1738.

125. *Vishwakarma R. G.* A Study of Angular Size-Redshift Relation for Models in Which Λ Decays as the Energy Density // Class. Quant. Grav. 2000. V. 17. P. 3833.

126. *Thorne K. S.* Primordial Element Formation, Primordial Magnetic Fields, and the Isotropy of the Universe // Astrophys. J. 1967. V. 148. P. 51–68.

127. *Kantowski R., Sachs R. K.* Some Spatially Homogeneous Anisotropic Relativistic Cosmological Models // J. Math. Phys. 1966. V. 7. P. 443–446.

128. *Kristian J., Sachs R. K.* Observations in Cosmology // Astrophys. J. 1966. V. 143. P. 379–399.

129. *Collins C. B., Glass E. N., Wilkinson D. A.* Exact Spatially Homogeneous Cosmologies // Gen. Rel. Grav. 1980. V. 12. P. 805–823.

130. *Gunn J., Tinsley B. M.* An Accelerating Universe // Nature. 1975. V. 257. P. 454–457.

131. *Wampler E. J., Burke W. L.* Cosmological Models with Nonzero Lambda // New Ideas in Astronomy. Cambridge Univ. Press, 1988. P. 317–326.

132. *MacCallum M. A. H.* A Class of Homogeneous Cosmological Models. III. Asymptotic Behaviour // Commun. Math. Phys. 1971. V. 20. P. 57–84.

133. *Koivisto T., Mota D. F.* Accelerating Cosmologies with an Anisotropic Equation of State // Astrophys. J. 2008. V. 679. P. 1–5.

134. *Mota D. F. et al.* Constraining Dark Energy Anisotropic Stress // Mon. Not. Roy. Astron. Soc. 2007. V. 382. P. 793–800.

135. *Saha B.* Some Remarks on Bianchi Type-II, VIII and IX Models // Grav. and Cosm. 2013. V. 19. P. 65–69.

136. *Astier P. et al.* The Supernova Legacy Survey: Measurement of Ω_M, Ω_Λ, and w from the First-Year Data Set // Astron. Astrophys. 2006. V. 447. P. 31.

137. *Garnavich P. M. et al.* Constraints on Cosmological Models from Hubble Space Telescope Observations of High-z Supernovae // Astrophys. J. 1998. V. 493. P. L53–L57.

138. *Garnavich P. M. et al.* Supernova Limits on the Cosmic Equation of State // Astrophys. J. 1998. V. 509. P. 74–79.

139. *Riess A. G. et al.* New Hubble Space Telescope Discoveries of Type Ia Supernovae at $z > 1$: Narrowing Constraints on the Early Behavior of Dark Energy // Astrophys. J. 2007. V. 659. P. 98–121.

140. *Riess A. G.* The Case for an Accelerating Universe from Supernovae // Publ. Astron. Soc. Pac. 2000. V. 112. P. 1284.

141. *Schmidt B. P. et al.* The High-z Supernova Search: Measuring Cosmic Deceleration and Global Curvature of the Universe Using Type Ia Supernovae // Astrophys. J. 1998. V. 507. P. 46–63.

142. *Saha B., Amirhashchi H., Pradhan A.* Two-Fluid Scenario for Dark Energy Models in an FRW Universe-Revisited // Astrophys. Space Sci. 2012. V. 342. P. 257–267.

143. *Padmanabhan T., Roychowdhury T.* A Theoretician's Analysis of the Supernova Data and the Limitations in Determining the Nature of Dark Energy // Mon. Not. Roy. Astron. Soc. 2003. V. 344. P. 823–834.

144. *Amendola L.* Acceleration at $z > 1$? // Ibid. V. 342. P. 221–226.

145. *Riess A. G. et al.* The Farthest Known Supernova: Support for an Accelerating Universe and a Glimpse of the Epoch of Deceleration // Astrophys. J. 2001. V. 560. P. 49–71.

146. *Caldwell R. R., Kamionkowski M., Weinberg N. N.* Phantom Energy: Dark Energy with $\omega < -1$ Causes a Cosmic Doomsday // Phys. Rev. Lett. 2003. V. 91. P. 071301.

147. *Dabrowski M. P., Stachowiak T., Szydlowski M.* Phantom Cosmologies // Phys. Rev. D. 2003. V. 68. P. 103519.

148. *Spergel D. N. et al.* First-Year Wilkinson Microwave Anisotropy Probe (WMAP) Observations: Determination of Cosmological Parameters // Astrophys. J. Suppl. 2003. V. 148. P. 175–194.

149. *Spergel D. N. et al.* Wilkinson Microwave Anisotropy Probe (WMAP) Three-Year Results: Implications for Cosmology // Astrophys. J. Suppl. 2007. V. 170. P. 377.

150. *Bennett C. L. et al.* Nine-Year Wilkinson Microwave Anisotropy Probe (WMAP) Observations: Final Maps and Results. arXiv:astro-ph.CO/1212.5225.

151. *Hinshaw G. et al.* Nine-Year Wilkinson Microwave Anisotropy Probe (WMAP) Observations: Cosmological Parameter Results. arXiv:astro-ph.CO/1212.5226.

152. *Chiba T., Nakamura T.* The Luminosity Distance, the Equation of State, and the Geometry of the Universe // Prog. Theor. Phys. 1998. V. 100. P. 1077–1082.

153. *Sahni V.* Exploring Dark Energy Using the Statefinder. arXiv:astro-ph/0211084.

154. *Blandford R. D. et al.* Cosmokinetics. arXiv:astro-ph/0408279.

155. *Visser M.* Jerk, Snap and the Cosmological Equation of State // Class. Quant. Grav. 2004. V. 21. P. 2603.

156. *Visser M.* Cosmography: Cosmology without the Einstein Equations // Gen. Rel. Grav. 2005. V. 37. P. 1541–1548.

157. *Rapetti D. et al.* A Kinematical Approach to Dark Energy Studies // Mon. Not. Roy. Astron. Soc. 2007. V. 375. P. 1510–1520.

158. *Bergmann P. G.* Comments on the Scalar-Tensor Theory // Intern. J. Theor. Phys. 1968. V. 1. P. 25–36.

159. *Wagoner R. V.* Scalar-Tensor Theory and Gravitational Waves // Phys. Rev. D. 1970. V. 1. P. 3209–3216.

160. *Zeldovich Ya. B.* The Cosmological Constant and the Theory of Elementary Particles // Sov. Fiz. Usp. 1968. V. 11. P. 381.

161. *Caroll S. M., Press W. H., Turner E. L.* The Cosmological Constant // Ann. Rev. Astron. Astrophys. 1992. V. 30. P. 499–542.

162. *Abdussattar and Vishwakarma R. G.* A Model of the Universe with Decaying Vacuum Energy // Pramana J. Phys. 1996. V. 47. P. 41–55.

163. *Peebles P. J. E., Ratra B.* The Cosmological Constant and Dark Energy // Rev. Mod. Phys. 2003. V. 75. P. 559–606.

164. *Padmanabhan T.* Cosmological Constant — the Weight of the Vacuum // Phys. Rep. 2003. V. 380. P. 235–320.

165. *Padmanabhan T.* Dark Energy and Gravity // Gen. Rel. Grav. 2008. V. 40. P. 529–564.

166. *Pradhan A.* Accelerating Dark Energy Models with Anisotropic Fluid in Bianchi Type-VI$_0$ Space-Time // Res. Astron. Astrophys. 2013. V. 13. P. 139–158.

167. *Virey J. M. et al.* Determination of the Deceleration Parameter from Supernovae Data // Phys. Rev. D. 2005. V. 72. P. 061302.